CHARACTERIZATION AND MODELING OF THORACO-ABDOMINAL RESPONSE TO BLAST WAVES

Volume 8. Effect of Clothing on Thoracic Response

Annual/Final Report

May 1985

James H.-Y. Yu
Edward J. Vasel
Cheng J. Chuong
James H. Stuhmiller, Principal Investigator

JAYCOR
11011 Torreyana Road
San Diego, California 92121

Contract No. DAMD17-82-C-2062

Supported by

U. S. Army Medical Research and Development Command
Fort Detrick, Frederick, Maryland 21701

The findings in this report are not to be construed as an official Department of the Army position unless so designated by other authorized documents.

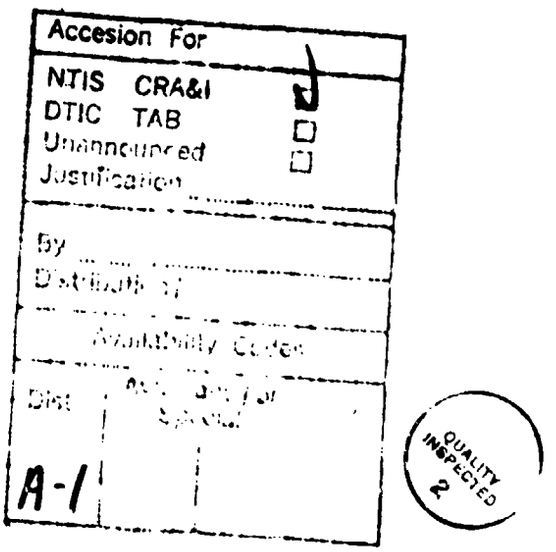

SECURITY CLASSIFICATION OF THIS PAGE

ADA190813

REPORT DOCUMENTATION PAGE

Form Approved
OMB No. 0704-0188

1a. REPORT SECURITY CLASSIFICATION UNCLASSIFIED	1b. RESTRICTIVE MARKINGS
2a. SECURITY CLASSIFICATION AUTHORITY	3. DISTRIBUTION/AVAILABILITY OF REPORT Approved for public release; distribution unlimited
2b. DECLASSIFICATION/DOWNGRADING SCHEDULE	
4. PERFORMING ORGANIZATION REPORT NUMBER(S)	5. MONITORING ORGANIZATION REPORT NUMBER(S)
6a. NAME OF PERFORMING ORGANIZATION JAYCOR 6b. OFFICE SYMBOL (If applicable)	7a. NAME OF MONITORING ORGANIZATION
6c. ADDRESS (City, State, and ZIP Code) 11011 Torreyana Road San Diego, California 92121	7b. ADDRESS (City, State, and ZIP Code)
8a. NAME OF FUNDING/SPONSORING ORGANIZATION U.S. Army Medical Research & Development Command 8b. OFFICE SYMBOL (If applicable)	9. PROCUREMENT INSTRUMENT IDENTIFICATION NUMBER DAMD17-82-C-2062
8c. ADDRESS (City, State, and ZIP Code) Fort Detrick Frederick, Maryland 21701-5012	10. SOURCE OF FUNDING NUMBERS PROGRAM ELEMENT NO. 61102A; PROJECT NO. 3M1 61102BS10; TASK NO. CG; WORK UNIT ACCESSION NO. 087

11. TITLE (Include Security Classification)
(U) Characterization and Modeling of Thoraco-Abdominal Response to Blast Waves
Volume 8. Effect of Clothing on Thoracic Response

12. PERSONAL AUTHOR(S) James H.-Y. Yu, E. Vasel, C. J. Chuong, and James H. Stuhmiller

13a. TYPE OF REPORT	13b. TIME COVERED	14. DATE OF REPORT (Year, Month, Day)	15. PAGE COUNT
Annual/Final	FROM 2/15/82 TO 5/31/85	1985 May	74

16. SUPPLEMENTARY NOTATION
Annual covers time period of 15 February 1984 - 31 May 1985.
Annual/Final published in 8 volumes

17. COSATI CODES			18. SUBJECT TERMS (Continue on reverse if necessary and identify by block number)
FIELD	GROUP	SUB-GROUP	
06	21		
06	17		

19. ABSTRACT (Continue on reverse if necessary and identify by block number)

20. DISTRIBUTION/AVAILABILITY OF ABSTRACT ☐ UNCLASSIFIED/UNLIMITED ☒ SAME AS RPT. ☐ DTIC USERS	21 ABSTRACT SECURITY CLASSIFICATION Unclassified
22a. NAME OF RESPONSIBLE INDIVIDUAL Mary Frances Bostian	22b. TELEPHONE (Include Area Code) 301-663-7325 22c. OFFICE SYMBOL SGRD-RMI-S

DD Form 1473, JUN 86 Previous editions are obsolete. SECURITY CLASSIFICATION OF THIS PAGE

FOREWORD

This Annual/Final Report has eight volumes. The titles are as follows:

1. Project Summary
2. Blast Load Definition on a Torso Model
3. Lung Dynamics and Mechanical Properties Determination
4. Biomechanical Model of Thorax Response to Blast Loading
5. Experimental Investigation of Lung Injury Mechanism
6. Biomechanical Model of Lung Injury Mechanisms
7. Gastrointestinal Response to Blast
8. Effect of Clothing on Thoracic Response

CONTENTS

Page

I. FINITE ELEMENT MODELING

1. BACKGROUND 1

2. FINITE ELEMENT MODELING 3

3. SUMMARY 11

4. REFERENCES 13

II. EXPERIMENTAL STUDY

1. INTRODUCTION 15

2. KEVLAR JACKET MATERIAL PROPERTIES 17

3. DYNAMIC RESPONSE OF KEVLAR FABRIC 25

3.1 Experimental Facility 25

3.2 Swatch Sample Tests 31

3.2.1 Test Sample Preparation 31

3.2.2 Swatch Test Results 35

3.3 Mannequin Test 46

3.3.1 Model Preparation 46

3.3.2 Mannequin Test Results 46

4. ONE DIMENSIONAL MODEL OF THE LUNG AND CHEST WALL COMPOSITE STRUCTURE 57

4.1 Introduction 57

4.2 Lung and Chest Wall Model Material Selection 57

4.3 Intrathoracic Pressure Measurements 64

4.4 Acceleration Measurement 67

ILLUSTRATIONS

Page

I. FINITE ELEMENT MODELING

1. Finite element modeling of clothing effect due to vest 4

2. Model ITP responses at various covering vest bulk moduli 5

3. Model ITP responses at various covering vest shear moduli 6

II. EXPERIMENTAL STUDY

1. PASGT vest 18

2. Specific tensile strength and specific tensile modulus of reinforcing fibers 19

3. Stress-strain behavior of yarns 20

4. Kevlar 29 fabric static loading test setup 22

5. Pressure-volume relationship of 30 layers of 2" × 2" Kevlar 29 swatch 24

6. Blast pressure from a powder actuated impactor as measured at the end of a 6 in. pipe without signal conditioning 26

7. Internal construction of the shock tube conditioning chamber 28

8. (a) JAYCOR 4" shock tube; (b) Face-on pressure signal with transducer directly exposed to the blast 29

9. Face-on POP signal 30

10. Side-on pressure signal 30

11. Effect of fabric coverage on face-on pressure signals 32

12. Kevlar swatch test samples 33

13. Test sample mounting arrangement 34

14. Target plate with relief holes surrounding the transducer 34

15. Pressure variation under different layers of Kevlar swatch for a given blast loading 36

Page

16. Pressure variation under different layers of cloth swatch for a given blast loading 37

17. Pressure variation versus blast pressure for a 20 layer Kevlar swatch 38

18. Pressure variation versus input blast pressure for a 30 layer cloth swatch 39

19. Pressure variation under Kevlar swatch as a function of number of layers 40

20. Pressure variation under layered cloth swatch vs side-on pressure as a function of number of layers 41

21. Pressure variation under Kevlar swatch vs number of layers for different pressure levels 42

22. Pressure variation under cloth swatch vs number of layers for different pressure levels 43

23. Pressure variation versus input blast pressure as measured under a Kevlar jacket over a flat plate 44

24. Force measurement results 45

25. Pressure measurement on bare mannequin 47

26. Pressure measurement on mannequin with Kevlar jacket 48

27. Pressure measurement on mannequin. A lab coat and a T-shirt are shown under the Kevlar jacket 49

28. Pressure variation measured on bare mannequin 50

29. Pressure variation measured under Kevlar jacket 51

30. Pressure variation measured on a mannequin; a lab coat and a T-shirt were worn under the Kevlar jacket 52

31. Pressure measurement on mannequin 53

32. Effect of Kevlar jacket on mannequin chest wall pressure 55

33. Velocity of wave in lung as measured by Fung and Yen 59

34. Water chamber used for wave speed measurement 61

35. (a) Pressure traces for wave speed measurements; (b) The signals greatly expanded in time for better resolution 62

Page

36. Wave speed measurements with and without auxiliary water chamber 63

37. Pressure trace under a one-dimensional lung and chest wall model 65

38. Effect of Kevlar fabric on pressure signal under lung and chest wall model material 66

39. Accelerometer measurement installations 68

40. Effect of Kevlar swatch on chest wall acceleration 69

41. Pressure trace under Kevlar swatch vs swatch surface acceleration 70

TABLES

Page

I. FINITE ELEMENT MODELING

1. Clothing Effects from WRAIR Volunteer Experiments 2

2. Model ITP Prediction on the Clothing Effect 8

II. EXPERIMENTAL STUDY

1. Comparative Properties 21

2. Velocity of Sound in Various Tissues, Air and Water 58

I. FINITE ELEMENT MODELING

1. BACKGROUND

Blast waves are known to cause injuries to internal organs, e.g., lung, gastrointestinal tract, ear, and larynx. To explore the possibility of using body covering as a means of protection, Clemedson and Jönsson [1] covered rabbits with rigid and soft material and exposed the animals to blast waves in shock tube and free field explosion experiments. They found that the rigid material protected the animal from lung injury. The soft coverings, however, were found to produce increased loading and aggravate the lung injury. Both peak pressure and rate of pressure rise in the thorax were found to be considerably higher in their experiments. Nevertheless the underlying mechanism causing such phenomena was not explained.

Volunteer experiments conducted by WRAIR showed increased peak intrathoracic pressure (ITP) on subjects wearing Kevlar vests. A set of data is shown in Table 1. For a 1 psig free field blast wave the peak ITP response increased from 0.394 to 0.440 psig, 11.7%, for subjects wearing a Kevlar vest. No noticeable change in d(ITP)/dt was observed.

From these results it appears that material coverings can increase the blast loading at the body surface, which, in turn, can cause increased ITP and higher risk of blast injury. Since ITP has been correlated with the severity of blast injury, understanding of the effect of vest material on blast wave transmission, reflection, and absorption is an important step toward the design of a protecting device.

Table 1. Clothing Effects from WRAIR Volunteer Experiments (from Ref. 3)

Clothing	Subject	Max ITP (psig)	ITP Increase (%)	Max d(ITP)/dt (psi/ms)	d(ITP)/dt Increase (%)
		Clothing 1 psi, face-on, arms down			
Fatigues	Volunteers	0.394 ± 0.129		0.158 ± 0.083	
	Victor	0.273		0.198	
Fatigue jacket	Volunteers	0.442 ± 0.099	12.2	0.157 ± 0.076	~0
	Victor	0.277	1.4	0.189	-5.1
Kevlar vest	Volunteers	0.440 ± 0.099	11.7	0.154 ± 0.042	~0
	Victor	0.280	2.6	0.180	-9.1

2. FINITE ELEMENT MODELING

A finite element model for a sheep torso was developed to study the body response to external blast wave loadings [?]. It was shown to be an effective approach to the study of blast biology. This model is adopted in the current investigation to study the effect of coverings on the body's response to external blast.

A layer of 20 elements representing a covering vest is added to the outer surface of the sheep torso model and its effect on the model ITP response is examined, see Figure 1. The total model is defined by 153 nodal points and 142 elements. Effective mechanical properties of a Kevlar vest are not fully understood at this time; a parametric approach is used. Mechanical properties of the covering vest are varied and the changes in the ITP response are examined. A blast wave after an 8 lb TNT explosion at 21.3 ft is applied on the model for these comparisons. The results are summarized in the following:

Effect of Bulk Modulus, K_o. The shear modulus G_o is fixed at 1.0×10^4 dyne/cm^2. The bulk modulus K_o is varied to investigate its effect on the model ITP response. The result is shown on Figure 2. When K_o is equal to or larger than 1.0×10^6 dyne/cm^2 there is little change in the ITP response from the case without covering vest. As we reduce K_o to 1.0×10^5 dyne/cm^2 the peak ITP increases approximately 20%. The peak ITP response increases up to 43% when the K_o is 1.0×10^4 dyne/cm^2. Further decrease of K_o to 1.0×10^3 dyne/cm^2, however, does not increase peak ITP. Also note that the rarefaction becomes pronounced as K_o is of the order of 10^5 or less.

Corresponding to the reduction in K_o there is a delay in the ITP rise time. It is due to the longer time needed for the incident compression wave to travel across the covering layer. The rate of ITP increase, however, did not seem to show a distinct difference.

Effect of Shear Modulus, G_o. The bulk modulus of the covering vest is fixed at 1.0×10^5 dyne/cm^2 and the shear modulus G_o is varied to understand its effect on the model ITP response. The results are shown in Figure 3. When the G_o is equal to or larger than 1.0×10^6 dyne/cm^2, little difference in the

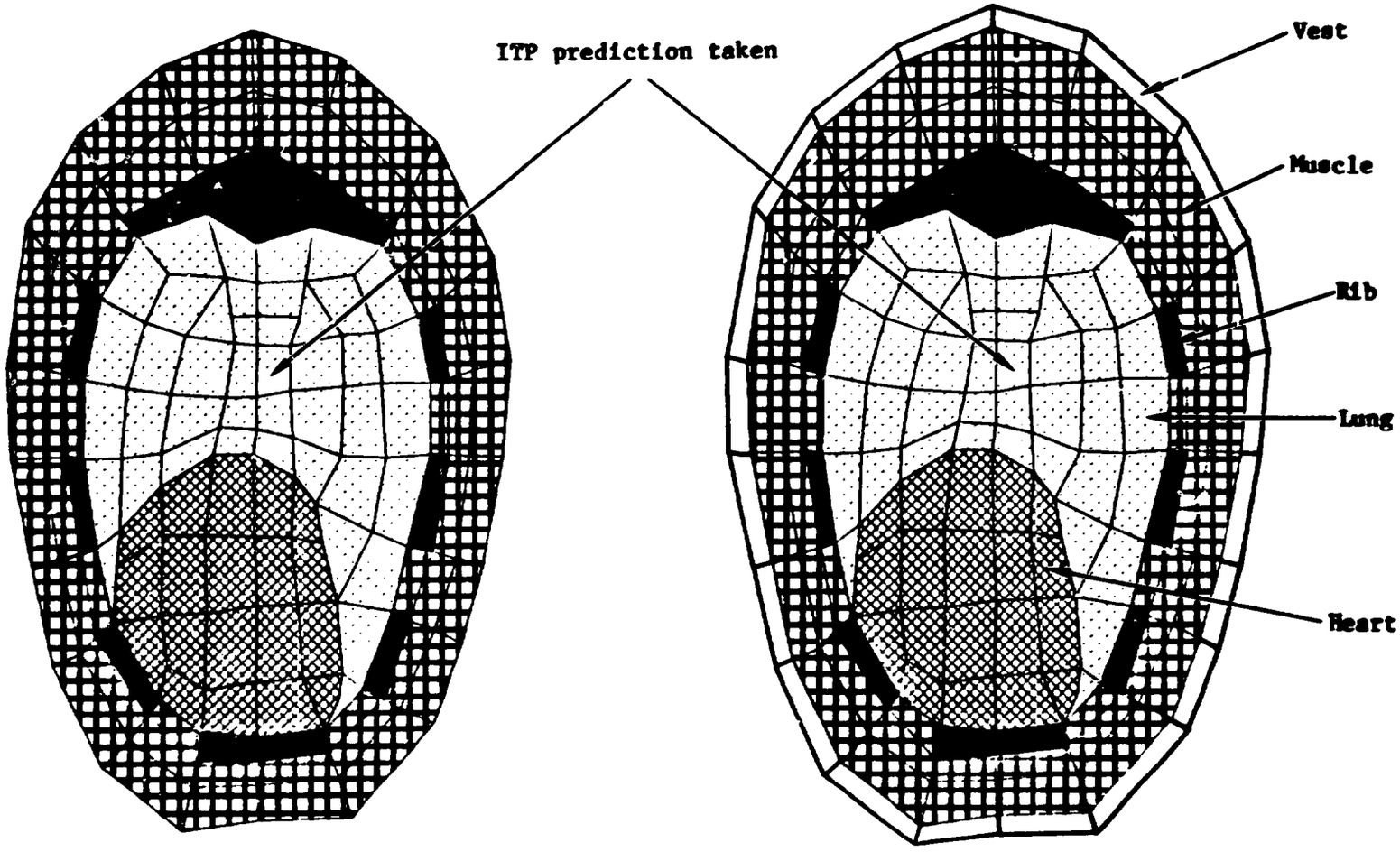

Figure 1. Finite element modeling of clothing effect due to vest

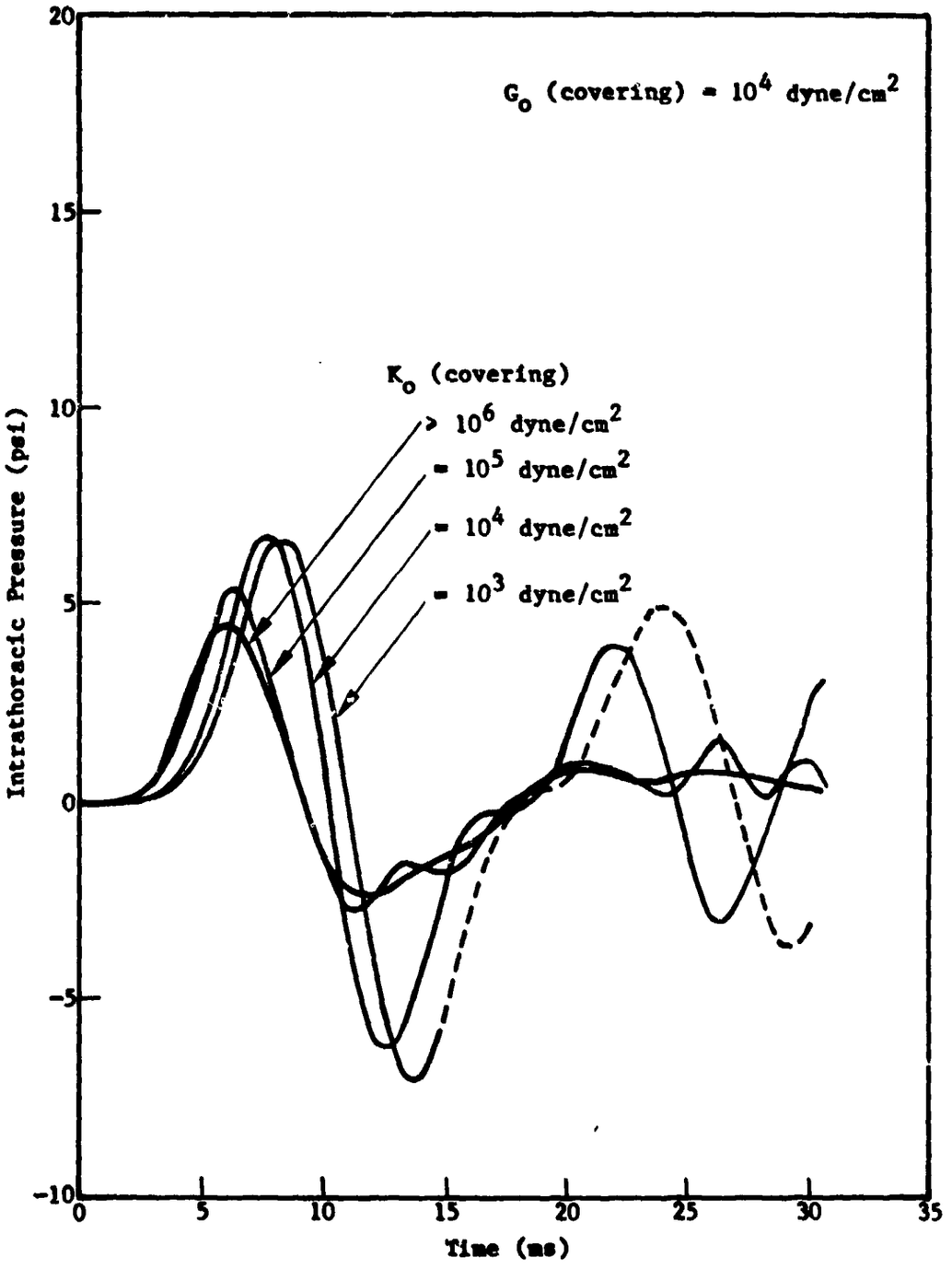

Figure 2. Model ITP responses at various covering vest bulk moduli, K_o

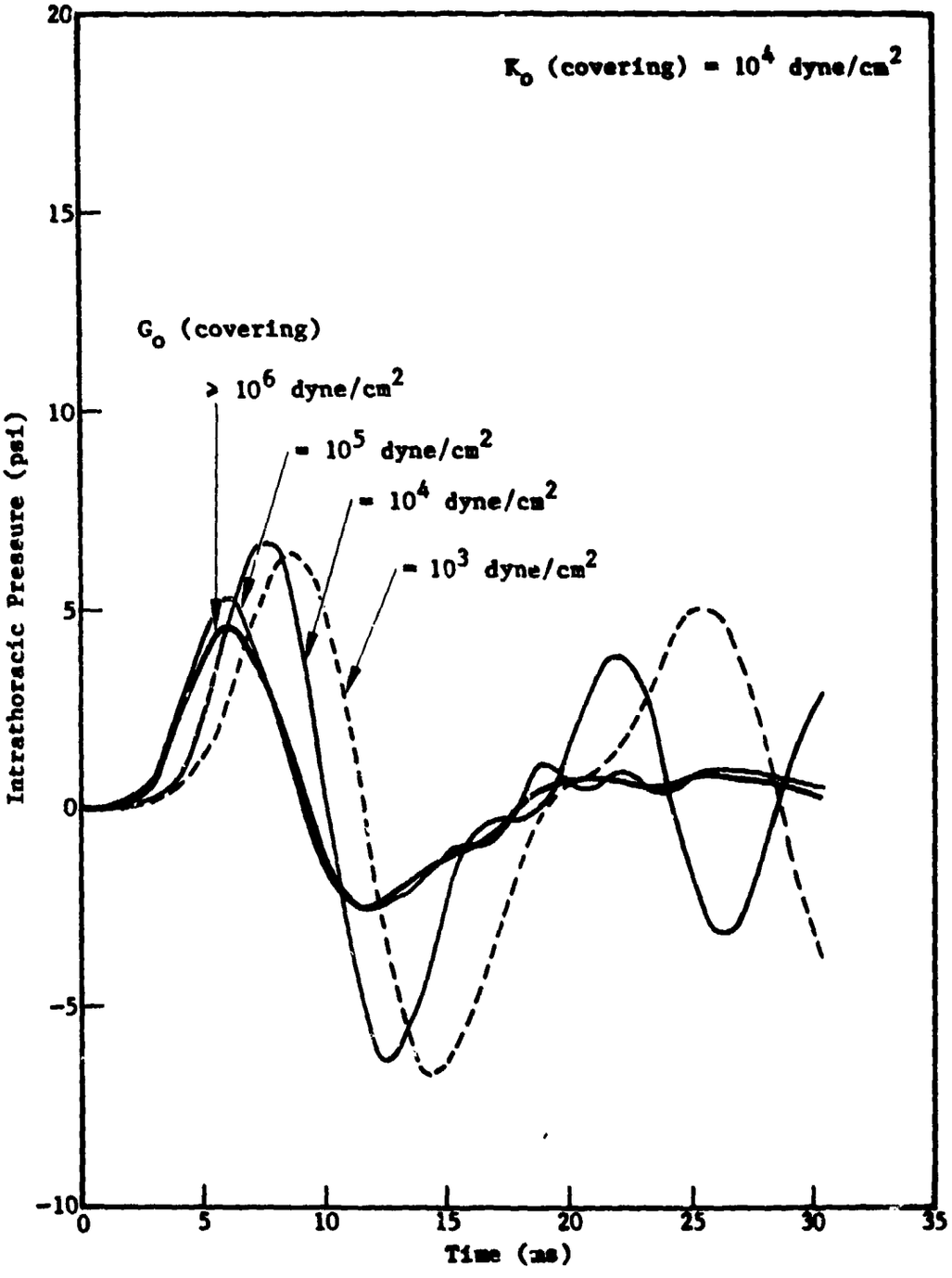

Figure 3. Model ITP responses at various covering vest shear moduli, G_o

ITP response can be seen from the case without covering vest. The peak ITP increases approximately 15% as we reduce the shear modulus G_o to 1.0×10^5 dyne/cm^2. The peak ITP increase reaches 43% as the G_o is reduced to 1.0×10^4 dyne/cm^2. Further reduction in G_o to 1.0×10^4 dyne/cm^2 does not lead to further change in peak ITP response.

The above studies also show that both bulk and shear moduli need to be of the order of 10^5 dyne/cm^2 or smaller to produce increased peak ITP response. From experience and observation, the shear modulus is a small number. It reflects th_ flexibility of the vest material. The effective bulk modulus of the vest appears to be the crucial one. The vest material is essentially a composite of woven Kevlar fibers and air. During the blast transient, part of the air can escape due to rapid compression. The above parametric study shows that if the effective bulk modulus of this material is 1.0×10^5 dyne/cm^2, it produces a 20% increase in peak ITP. Density measurement on the Kevlar swatch shows an average density of 0.6-0.75 g/cm^3. This suggests a low compression wave speed of approximately $c = (K/\rho)^{1/2} \approx 4$ m/sec. The low wave speed and the material impedance from the neighboring materials, air and skeletal muscle, may lead to the redistribution of wave energy and increased loading on the body surface. Further investigation of this is needed.

Clothing Effect at Various Blast Loadings. For a given blast wave, ITP is found to increase when the subject wears a spongy covering vest or clothing. The peak ITP percentage increase from the case without covering is used as an index to account for the clothing effect. Previous isoimpulse studies demonstrated that a higher peak blast wave can result in higher ITP response and thereby more severe injury. One would like to know if clothing effect becomes amplified at higher blast loading.

Loadings of Friedlander wave at different peak overpressures are applied on the model and their ITP responses are predicted. Three different peak blasts - 1, 8, and 45 psi - are applied on the model with and without coverings. Effective bulk and shear moduli of the covering vest are assumed to be 1.0×10^5 and 1.0×10^4 dyne/cm^2, respectively. Table 2 lists the model maximum ITP prediction and the maximum d(ITP)/dt for all three loading cases. It appears that both the percentage increases of the maximum ITP and the maximum d(ITP)/dt are insensitive to the variation of peak blast loadings delivered.

Table 2. Model ITP Prediction on the Clothing Effect

Loading (psi)	Model Description	Max ITP (psig)	ITP Increase (%)	Max d(ITP)/dt (psi/ms)	d(ITP)/dt Increase (%)
1	Without jacket	0.52		0.21	
	With jacket	0.63	21.2	0.27	29.0
8.	Without jacket	4.40		1.74	
	With jacket	5.38	22.0	2.31	32.0
45	Without jacket	23.4		9.2	
	With jacket	28.16	20.3	12.1	31.4

For the assumed vest material, the percentages of ITP increase fall in the neighborhood of 20% and those of the d(ITP)/dt increase are of the order of 30% when the peak blast overpressure varies from 1 to 45 psi.

3. SUMMARY

Various experiments demonstrate that a spongy covering can increase the body ITP response to external blast wave loading. A finite element model is used to study the clothing effect of various covering materials.

A parametric approach is used. The peak ITP increase percentage is used as an index to quantify the altered ITP response. For a 1 psi blast loading it is shown that a vest with effective bulk modulus of 2.0×10^5 dyne/cm^2 can produce 10% ITP increase from the case without covering on a sheep. This can be compared to the WRAIR volunteer experiment results of 11.7% increase on subjects wearing a Kevlar vest.

Loadings of Friedlander wave at different peak overpressure are applied on the model to see if the clothing effect depends on the magnitude of blast overpressure. The bulk and shear moduli of the vest are assumed to be 1.0×10^5 and 1.0×10^4 dyne/cm^2, respectively. The result shows that the clothing effect is rather insensitive to the magnitude of peak blast overpressure within 45 psi.

4. REFERENCES

1. Clemedson, C.-J., et al., "Effects on Extra- and Intrathoracic Pressure Pattern and Lung Injuries of Rigid and Soft Protection of Thorax in Air Blast Exposed Rabbits," Rörsvarsmedicin 7, 172-190 (1971).

2. Chuong, C. J. and J. H. Stuhmiller, "Characterization and Modeling of Thoraco-Abdominal Response to Blast Waves, Volume 4: Biomechanical Model of Thorax Response to Blast Loading," Final Report to WRAIR under Contract No. DAMD17-82-C-2062 (1985).

3. Phillips, Y. Y., J. J. Jaeger, and A. J. Young, "Biophysics of Injury from Repeated Blast," Proceedings of Tripartite Technology Coordinating Program Panel W-2, Muzzle Blast Overpressure Workshop, May 1982.

II. EXPERIMENTAL STUDY

1. INTRODUCTION

Previous field tests on volunteers wearing Kevlar vests and animal tests with thick coverings showed statistically higher intrathoracic pressure. The mechanisms that led to such results are unknown.

A series of experiments was carried out to study the phenomena. Sample Kevlar fabric was acquired from a vendor to determine its physical properties. For a stack of 30 layers of fabric under static loading, the bulk modulus was found to be about 1 psi or 6.89×10^4 dynes/cm^2. Depending on the amount of compression applied, the mass density of the sample was found to vary from an initial value of 0.6 to an asymptotic value of 0.747 gm/cm^3.

The dynamic response of the Kevlar fabric was tested by exposing sample Kevlar swatches to blast overpressure generated by a 4 inch shock tube. The samples were prepared by inserting various layers of fabric in cotton bags to simulate the construction of a Kevlar vest. There was a systematic trend of pressure increase under the test sample versus number of layers until a certain limit after which the peak pressure would decrease. Similar tests were conducted for the PASGT vest by mounting it over the flat target plate. It was found that the pressure response agreed quite well with the general trend of the swatch tests. A similar pressure-versus-layer trend was found for regular cotton swatches. Such results led us to believe that the layered structure, in addition to material compressibility, could be the primary cause of blast pressure amplification.

Two special materials, a closed-cell double skin neoprene and a hard rubber, were found to have wave speeds similar to those of the lung and intercostal muscle, respectively. A physical model using these materials was fabricated to study the possible ITP response under blast loading. Under this model the blast signal was highly damped, unlike the biological system, so that no noticeable difference was detected for the conditions of with and without Kevlar swatch coverings.

2. KEVLAR JACKET MATERIAL PROPERTIES

According to MIL-C-44050, the ballistic aramid cloth used for the PASGT vests are made of Kevlar 29 fabric. A medium size PASGT vest (Fig. 1) was purchased from Gentex Corporation of Carbondale, Pennsylvania, to be used for later dynamic loading tests.

Material properties of the Kevlar 29 fiber were given by Du Pont Corporation. The tensile strength and the stress-strain relationship of the Kevlar 29 as compared to other material and yarns is shown in Figures 2 and 3. Some basic information with regard to the Kevlar fiber is summarized in Table 1.

For the swatch test, samples of Kevlar 29 plain weave fabrics were purchased from Hexcel Corporation of Dublin, California. Material properties provided by the vendor are listed below:

Fabric style	710
Yarn	1500 denier
Count	24 × 24
Thickness	0.017 inch
Weight	9.5 oz/sq yd
Tensile strength	
Warp	1100 lb/in.
Filling	1100 lb/in.

Density and a p-V relationship for the Kevlar 29 fabric were measured by using a stack of 30 layers of 2" × 2" Hexcel fabrics. The experimental setup is shown in Figure 4.

The height variation of the test sample was measured against the applied load. Since the areas of the test samples under static loading could be assumed constant, the height variation was used as the indicator of the volume change. Furthermore, since the height change is most pronounced at the initial loading stage, a graduated cylinder was used for small load increments by adding water to it.

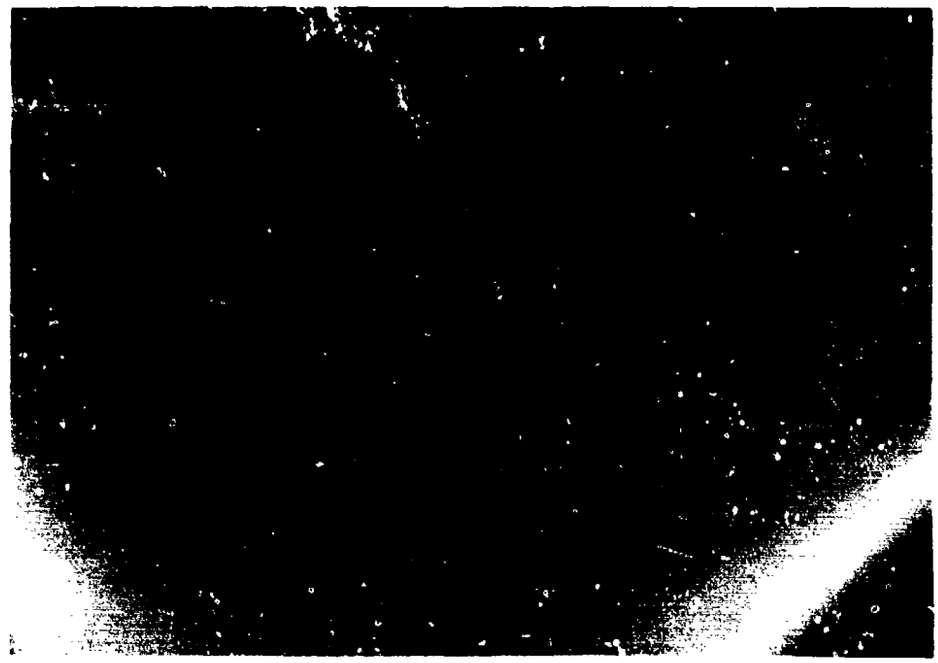

Figure 1. PASGT vest. There are 13 layers of plain weave Kevlar 29 fabric under the canvas cover.

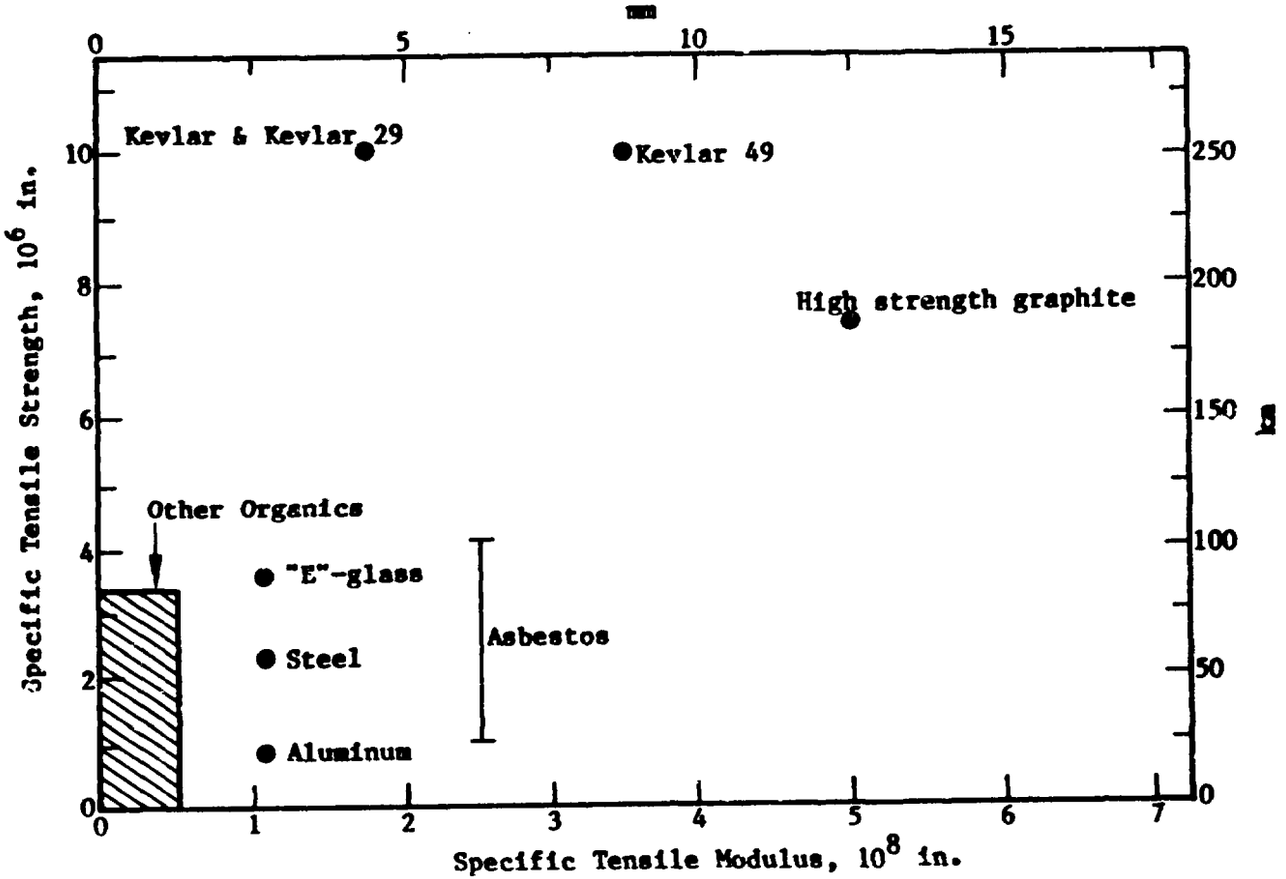

Figure 2. Specific* tensile strength and specific* tensile modulus of reinforcing fibers

Tested per resin impregnated strand test - ASTM D2343

*Tensile strength or modulus divided by density

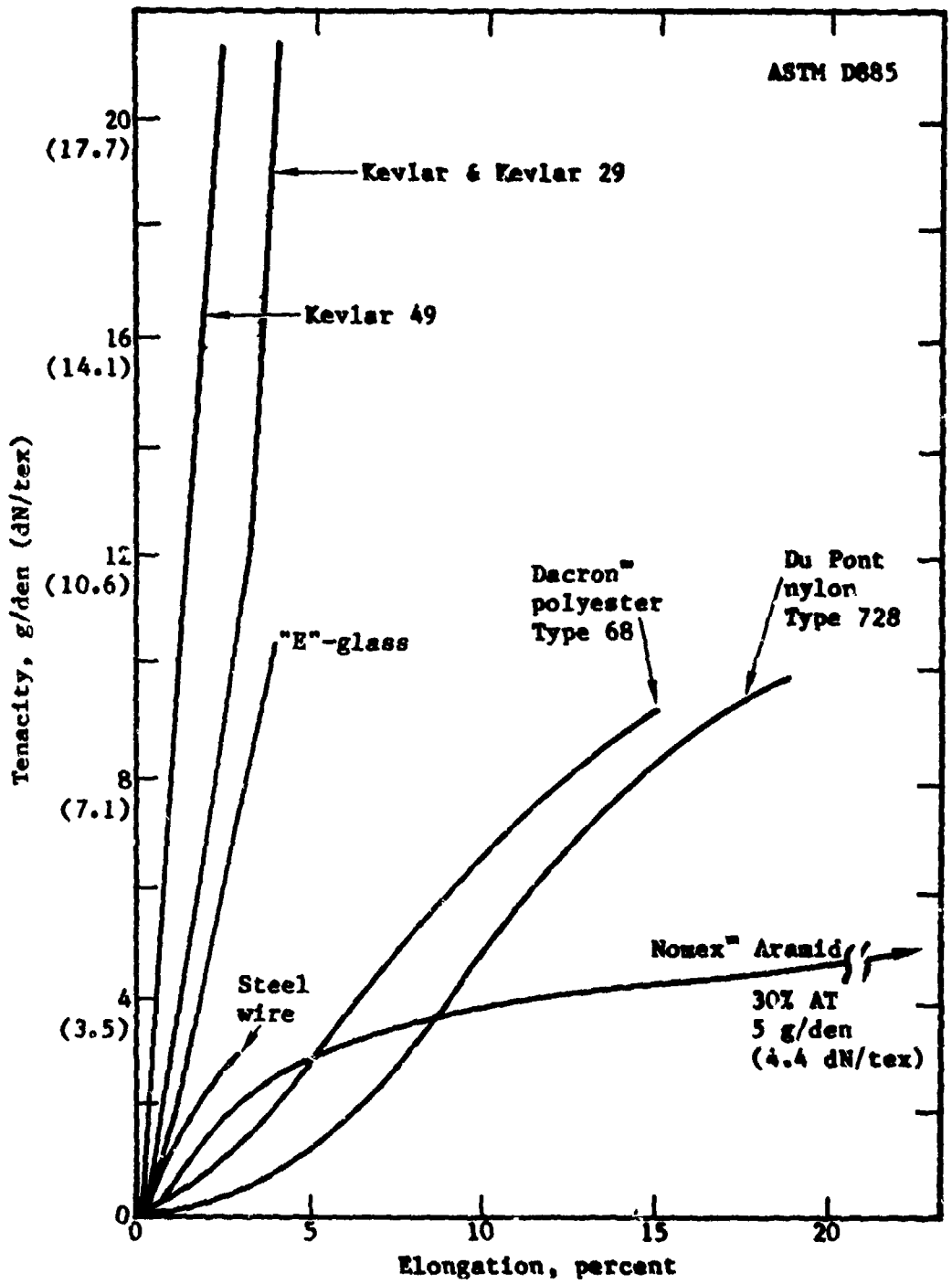

Figure 3. Stress-strain behavior of yarns (expressed in textile units)

Table 1. Comparative Properties

Material	Tensile Strength lb/in.^{2} (MPa)*	Tenacity g/den (dN/tex)	Modulus lb/in.^{2} (MPa)	Elongation at Break, (%)	Density lb/in.^{3} (g/cm^3)
Yarn - tested per textile test (ASTM D885)					
Kevlar 29	400,000 (2,760)	22 (19.4)	9,000,000 (62,000)	3.6	0.052 (1.44)
Kevlar 49	400,000 (2,760)	22 (19.4)	17,000,000 (117,000)	2.5	0.052 (1.44)
Du Pont Nylon (Type 728)	143,000 (985)	9.8 (8.6)	800,000 (5,520)	18.3	0.041 (1.14)
Dacron** polyester (Type 68)	162,500 (1,120)	9.2 (8.1)	2,000,000 (13,800)	14.5	0.050 (1.38)
Stainless steel	250,000 (1,720)	2.5 (2.2)	29,000,000 (200,000)	2.0	0.283 (7.83)
Reinforcing Fibers - tested per resin impregnated strand test (ASTM D2343)					
Kevlar 29	525,000 (3,620)		12,000,000 (83,000)	4.4	0.052 (1.44)
Kevlar 49	525,000 (3,620)		18,000,000 (124,000)	2.9	0.052 (1.44)
High strength graphite	450,000 (3,100)		32,000,000 (221,000)	1.25	0.063 (1.75)
"E"-Glass	350,000 (2,410)		10,000,000 (69,000)	3.5	0.092 (2.55)
Asbestos	100,000-400,000 (690-2,760)		23,200,0 (160,000)	0.4-1.7	0.090 (2.50)

*MPa = MN/m^2 = lb/in.^{2} × 6.895 × 10^{-3}

**Dacron is DuPont's registered trademark for its polyester fiber.

Figure 4. Kevlar 29 fabric static loading test setup.

The experimental result is shown in Figure 5. Notice the two markedly different slopes of the pressure volume curves: an initial high rate of volume change followed by a slow variation when $|\Delta v/v_o| > 0.16$ at a loading of about 0.5 psi. Also shown is the strong hysteresis during the unloading process. The linear portion of the calibration curve shows that the bulk modulus, K, of the Kevlar swatch is about 1 psi or 6.89×10^4 dynes/cm^2.

Using the unit weight of 9.5 oz/sq yd given by the vendor, density of the fabric calculated based on the measured thickness at both zero loading and asymptotic thickness at final loading (roughly the same thickness as given by the vendor) are:

$$(9.5/16)/(3 \times 3 \times 0.021/12) = 37.7 \text{ lb/cu ft}$$

$$(9.5/16)/(3 \times 3 \times 0.017/12) = 46.6 \text{ lb/cu ft}$$

The equivalent specific gravities based on the unit weights are then 0.604 and 0.747, respectively.

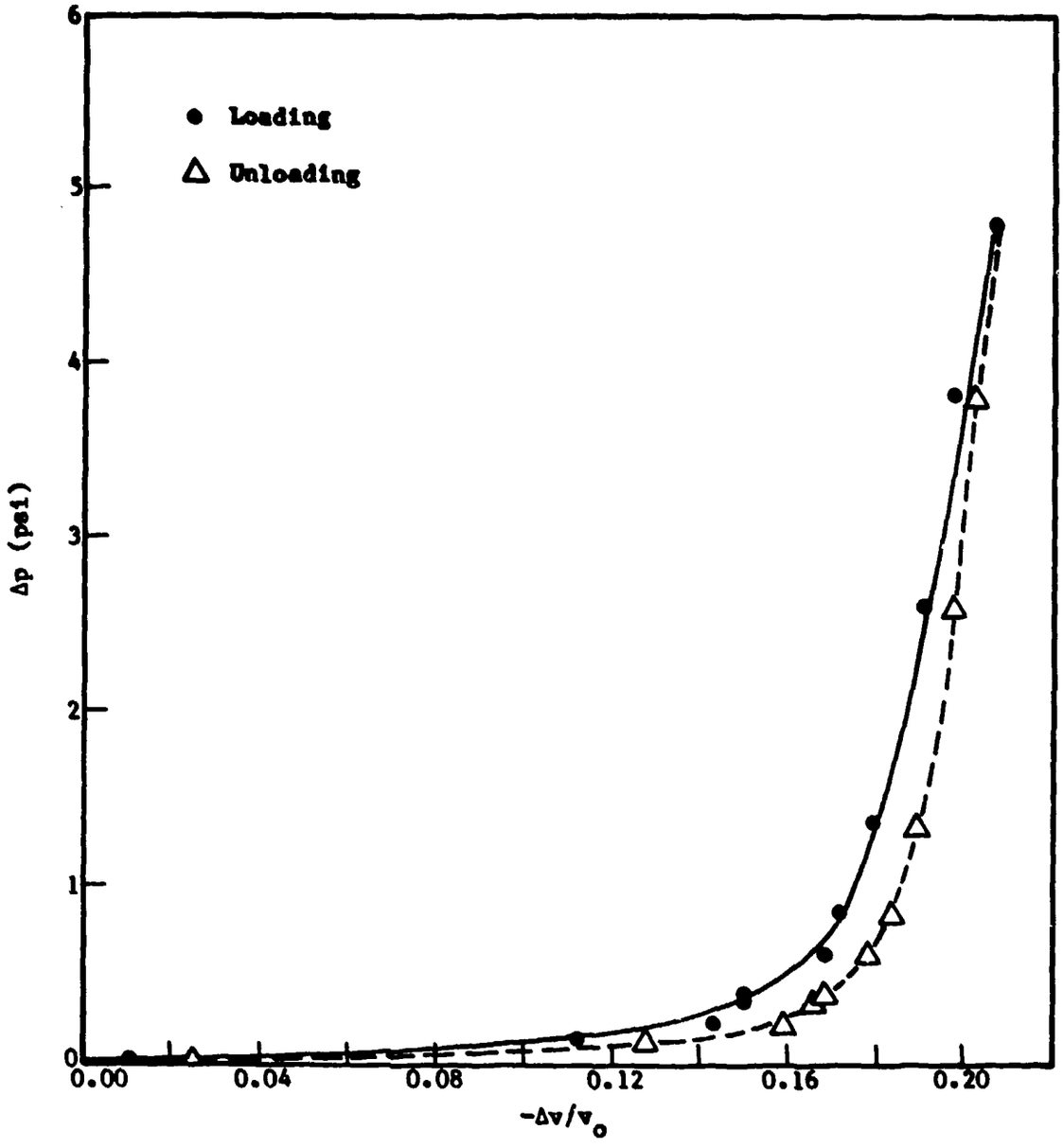

Figure 5. Pressure-volume relationship of 30 layers of 2" × 2" Kevlar 29 swatch

3. DYNAMIC RESPONSE OF KEVLAR FABRIC

The static properties found in Section 2 can be used in modeling of the jacket. In this section the setup, loading technique, and results of dynamic tests are described.

3.1 EXPERIMENTAL FACILITY

There were two considerations in the blast loading tests: the method of loading, and the approach of pressure measurement. A fast response pressure transducer installed on a target plate under the test sample was used for pressure measurement. Ample silicone grease was applied over the pressure transducer to ensure full pressure transfer from the test sample to the transducer.

Originally, a water jet impactor was to be used to provide the blast loading, but it was learned that when the Kevlar fabric was exposed to moisture its physical properties could be altered. The validity of the test results obtained with a water jet impactor would be questionable. To alleviate such uncertainty, an alternative loading approach using a powder actuated impactor was selected.

Since the impactor used gunpowder as propellant for its power loads, blast signals were generated at the muzzle. In principle, a large diameter pipe attached to the end of the muzzle would allow the blast signal to expand and provide us a uniform blast field for the Kevlar test. Preliminary tests, however, showed that the blast signal had the following defects: irregular and short in duration (see Fig. 6), pressure concentration around the center of the shock tube, and presence of ignition flame and blast debris at the shock tube exit.

To overcome these defects, the following approaches were taken. To increase the duration of the blast signal, a signal conditioning chamber was designed and installed immediately downstream of the muzzle. Since the duration of a pressure pulse depended on how fast the exhaust gas was released, a

(a) Pressure transducer covered by a single layer of cloth

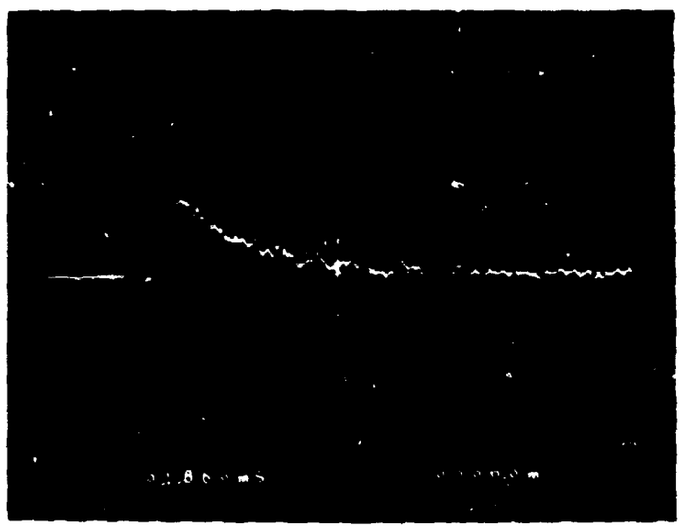

(b) Pressure transducer covered with two layers of cloth

Figure 6. Blast pressure signals from a powder actuated impactor as measured at the end of a 6 in. pipe without signal conditioning chamber

baffle plate with a relatively low opening ratio was installed. To avoid the blast concentration on the muzzle axis, a center piece blockage was installed on the baffle plate.

The blockage at the baffle plate would cause the pressure wave to reflect back toward the muzzle. A circular plate was installed on the plane of the muzzle to redirect the reflected pressure toward the baffle plate again. The reflections between the baffle plate and the muzzle plate would continue until all the exhaust gas generated by the blast was released downstream. The size of the conditioning chamber, distance between the baffle plate and the muzzle plate, and the opening ratio of the baffle plate dictate the uniformity and duration of the pressure signal at the exit. Figure 7 is a photograph of the internal construction of the conditioning chamber.

The power loads were filled with gunpowder and plugged with waxed paper wads. During blasts these paper wads would be expelled from the shock tube together with the ignition residues. Furthermore, ignition flames also accompany the gun blast. To prevent the burning of the test sample and the spreading of the debris over the target, stainless steel catcher screens were installed. One was directly in front of the baffle plate and three others at a station six inches further downstream. This arrangement was found to trap most of the blast residue and arrest the blast flame. The added flow restriction due to the catcher screens also made the pressure distribution at the shock tube exit more uniform. Pressure measurements traversed across the shock tube showed a very even pressure distribution. Figure 8(a) shows the final arrangement of the shock tube and Figure 8(b) is a typical face-on pressure signal.

The signals generated by this arrangement had longer durations and cleaner pressure traces than those obtained without the conditioning chamber. However, the pressure signals had very sharp pressure fronts. These sharp pressure fronts were caused by the thin shock layer ahead of the blast waves. Their values tended to vary significantly from shot to shot. A single layer of cloth installed over the pressure transducer absorbed most of the spurious and relatively small energy in the initial peaks. The result was a more repeatable signal that retains the bulk of the energy (Fig. 9).

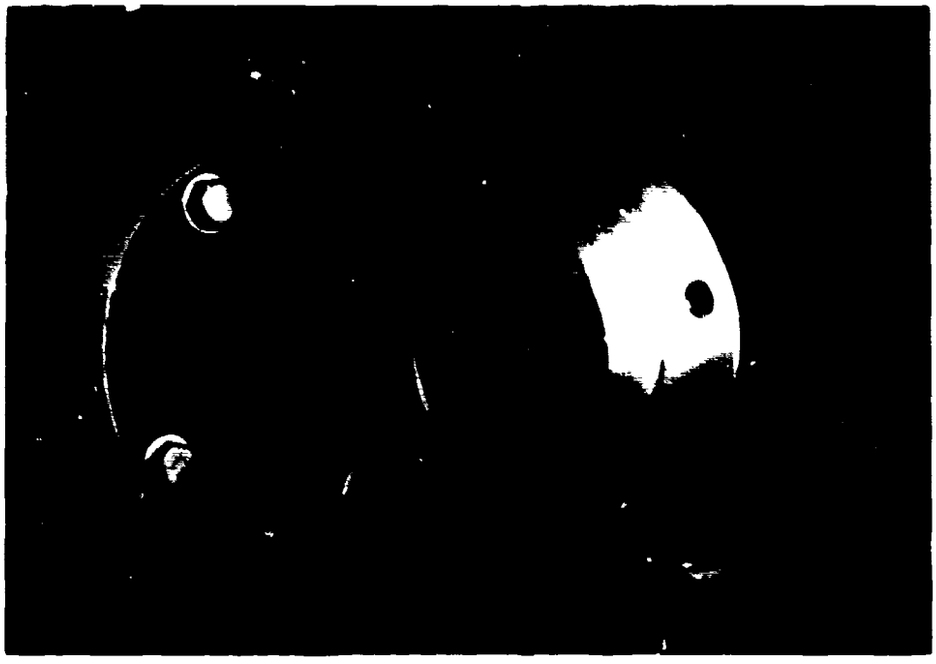

Figure 7. Internal construction of the shock tube conditioning chamber

Signal Conditioning Chamber

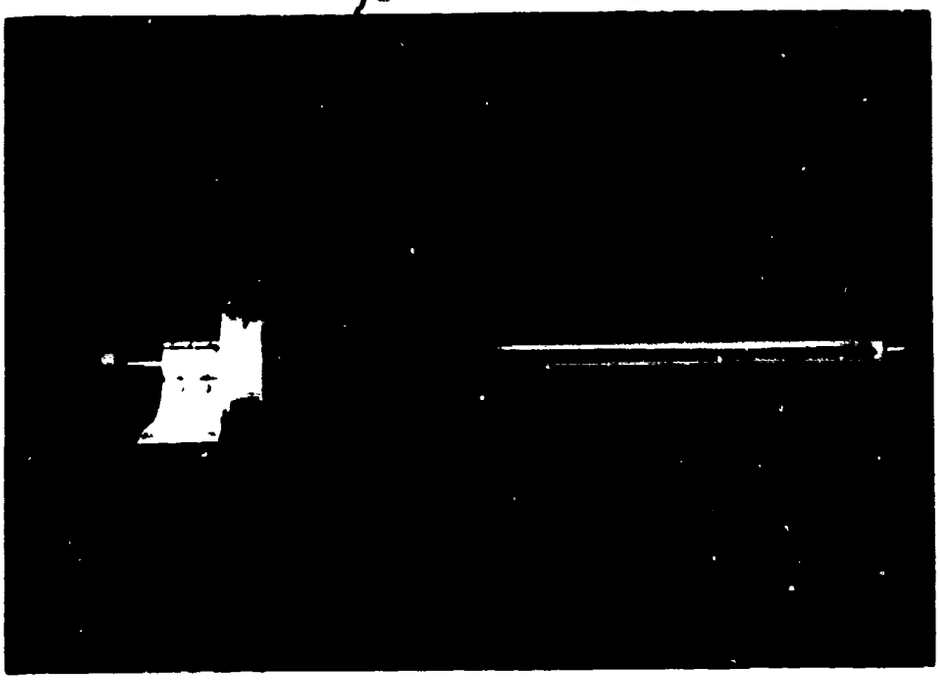

(a) JAYCOR 4 inch shock tube

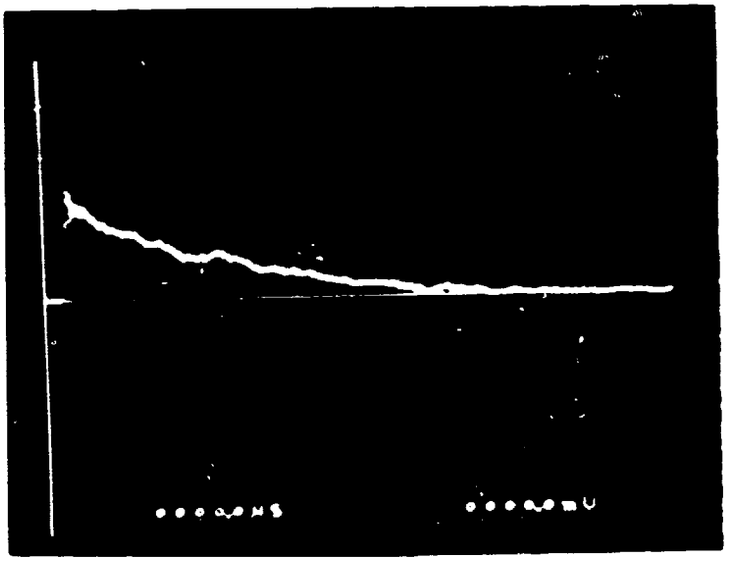

Figure 8 (b). Face-on pressure signal with transducer directly exposed to the blast

Figure 9. Face-on BOP signal. Rise time = 10 μs; peak pressue = 22 psi; A-duration = 3.3 ms

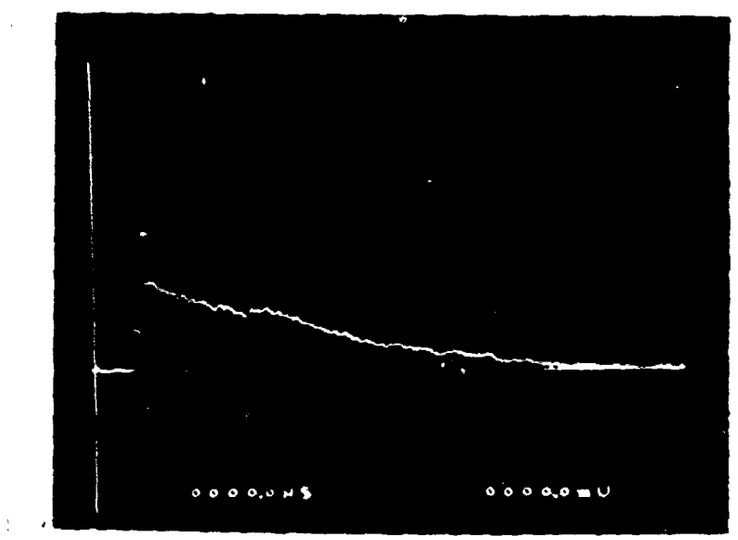

Figure 10. Side-on pressure signal. The pressure transducer was mounted on the shock tube wall 0.6 inch from the end cover plate. The value at the knee is the input blast pressure, and the peak is the reflected signal.

Since most blast-related work in the literature used side-on pressure as the reference, a pressure transducer was installed on the shock tube side wall (0.6 inch from the exit) to measure the input blast signal. Because the diameter of the pressure transducer is much larger than the thickness of the shock, the side-on transducer represented the actual integrated pressure during the passage of the blast wave. The result was a more uniform and consistent value. It was used as the reference for all subsequent tests. Figure 11 illustrates the effect of different layers of cloth coverage on the face-on pressure.

In free field tests, the pressure transducer measures the passage of the blast signal without reflected waves. In this series of tests, since the end of the test chamber was closed to increase the blast pressure, the side wall transducer would also measure the passage of the reflected pressure with its "doubling effect." Figure 10 shows a typical pressure signal measured by a side wall transducer.

3.2 SWATCH SAMPLE TESTS

3.2.1 Test Sample Preparation

To test the dynamic response of the Kevlar fabric, samples of 2" × 2" swatches were prepared. To simulate the construction of the PASGT vest, the test samples were prepared individually by inserting different numbers of layers into cotton fabric bags as shown in Figure 12.

These test samples were mounted on the target plate over the pressure transducer. To prevent blast pressure from coming directly from the gap between the test sample and the plate, the test samples were sealed around the periphery with tape (Fig. 13). As described earlier, ample silicone grease was applied over the pressure transducer to ensure full blast pressure transfer from the test sample to the pressure transducer.

Initial test results showed that such arrangement would trap air under the test specimen. During blast tests, the trapped air was not able to escape and the pressure signal represented the compression cycle of the trapped air rather than the true signal due to compression of the Kevlar specimen. Furthermore, without relief holes the trapped air under compression would occasionally cause the test samples to lose contact with the transducer and

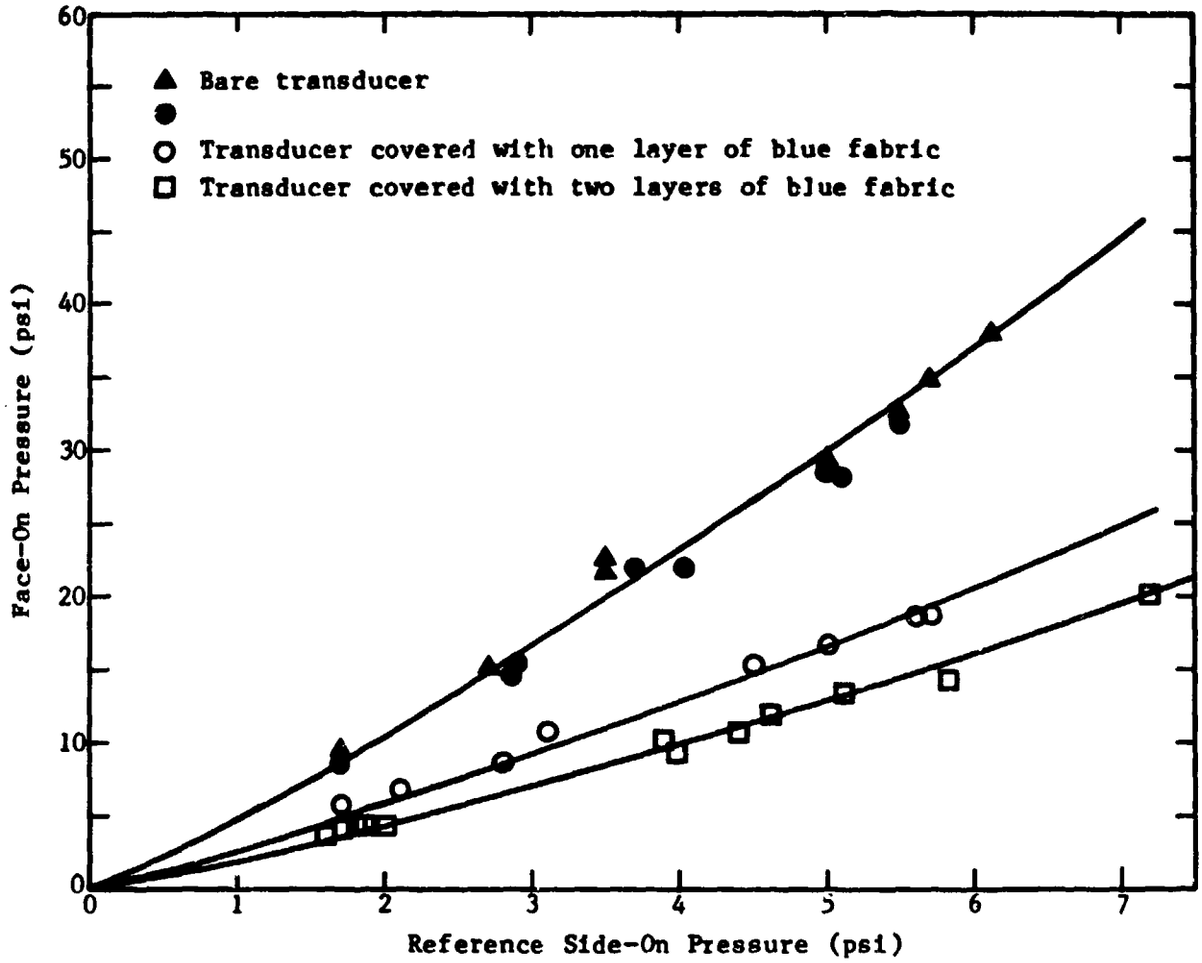

Figure 11. Effect of fabric coverage on face-on pressure signals

Figure 12. Kevlar swatch test samples. The test fabric was enclosed in the cotton fabric bags.

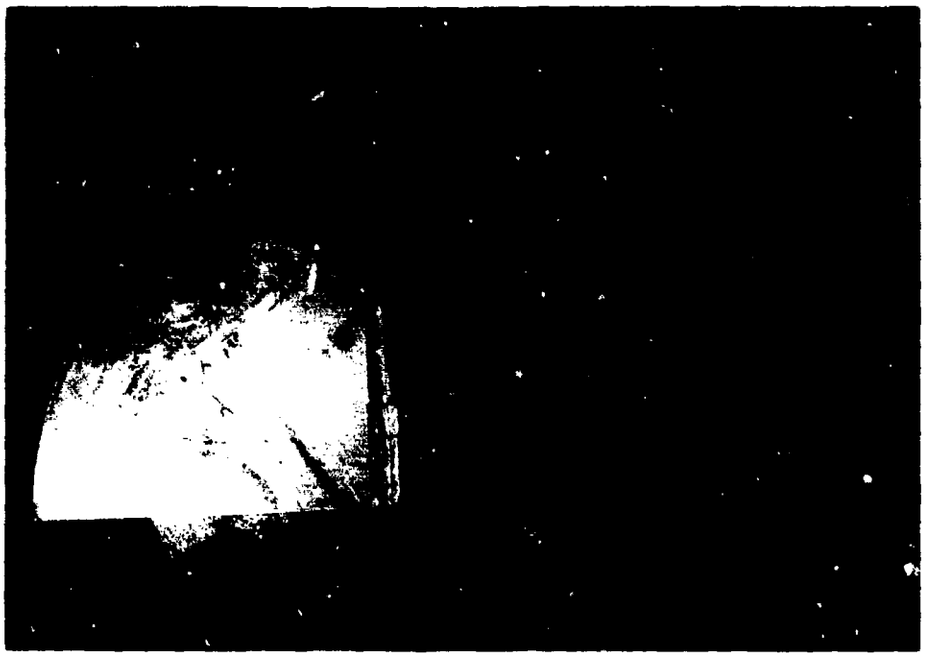

Figure 13. Test sample mounting arrangement

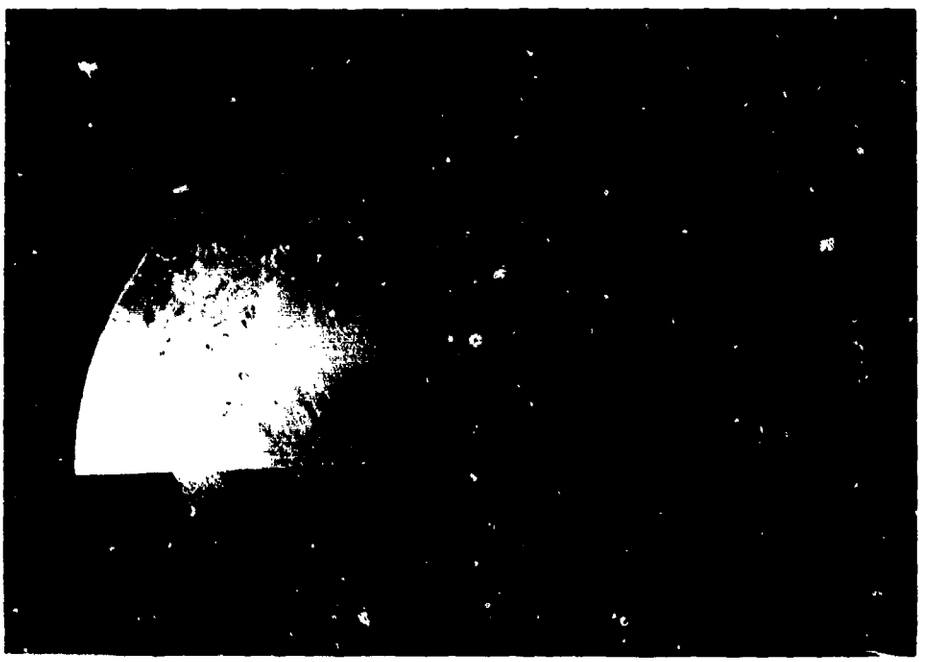

Figure 14. Target plate with relief holes surrounding the transducer

result in vastly different signals. To alleviate this problem, the target mounting plate was drilled with relief holes to allow air escape during blast (Fig. 14). This arrangement simulated more closely the condition of the vest where the air enclosed would escape around the periphery during blast. The test results obtained under these conditions were more consistent.

In order to identify the unique features associated with the Kevlar fabric, similarly constructed samples were prepared with regular blue cotton fabric. Identical test conditions were used to measure the pressure response for these samples and were compared with the Kevlar swatch test results.

3.2.2 Swatch Test Results

Figures 15 through 18 are the results of the swatch tests. P_o is the input side-on pressure, and P_m is the peak pressure under the swatch. Designations of 1T, 3T, etc. represent the number of test fabric layers in the bag, K stands for Kevlar and B for the (blue) cotton fabric. The results are summarized in Figures 19 and 20. They are replotted in Figures 21 and 22 in terms of number of layers for four different reference pressures.

These results clearly show that the pressure signals under multilayer fabrics tend to have much higher values. The pressure increase is in direct proportion to the number of layers until certain thicknesses were reached, after which the peak pressure decreased.

Though the effect was not as great as that of the Kevlar fabric, the cotton fabric exhibited similar layer versus pressure trends. When the PASGT vest was clamped to the target plate and exposed to the blast, a similar pressure result was obtained (Fig. 23). This result was in fair agreement with the general trend of swatch tests. The results were included in Figure 19 for comparison.

In order to verify that the observed signal enhancement was not a local anomaly of pressure measurement, a force transducer was acquired to measure the force under the whole test sample. In this case a 2 in. square target plate was used. A 25 TK test sample was then mounted on the target and the total force under blast was measured. Figure 24 shows the results for the test conditions with and without the Kevlar swatch. Again, when the target was

(1) 1 TK, P_o = 4.9 psi, P_m = 16.4 psi

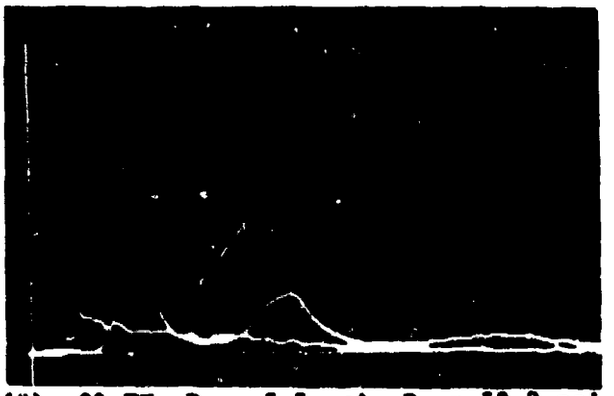

(5) 20 TK, P_o = 5.5 psi, P_m = 52.2 psi (Vertical scale doubled)

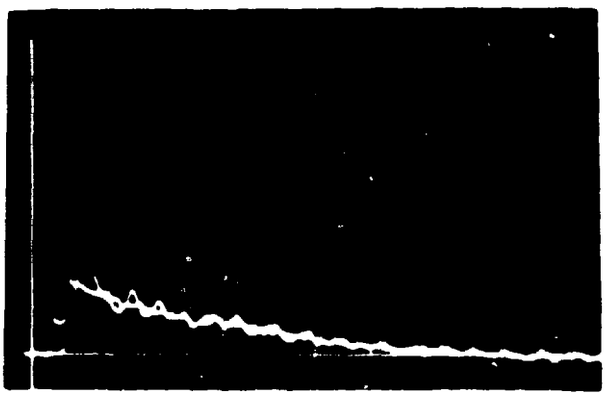

(2) 3 TK, P_o = 5.5 psi, P_m = 32.2 psi

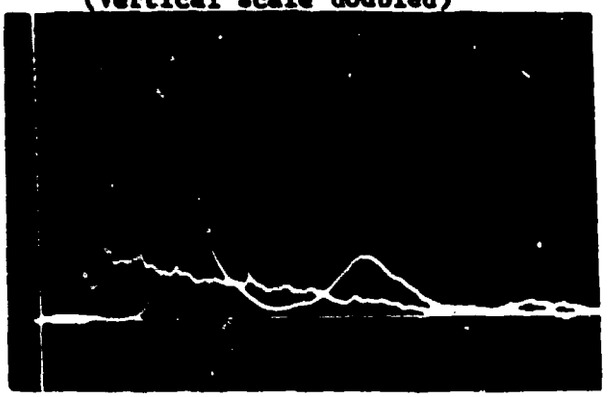

(6) 25 TK, P_o = 5.2 psi, P_m = 37.4 psi

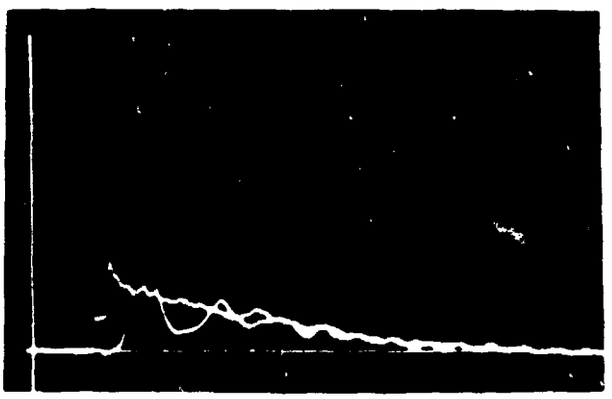

(3) 10 TK, P_o = 5.2 psi, P_m = 34.5 psi

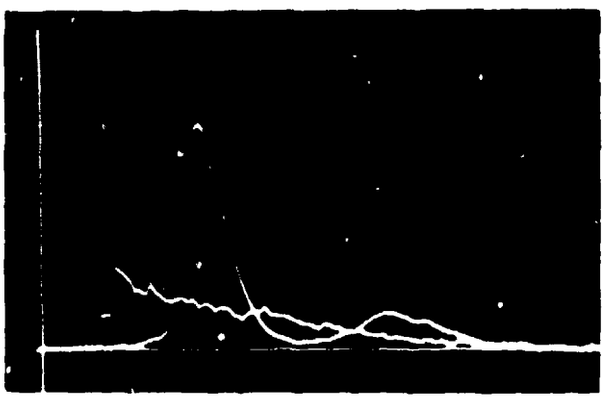

(7) 30 TK, P_o = 5.2 psi, P_m = 31.5 psi

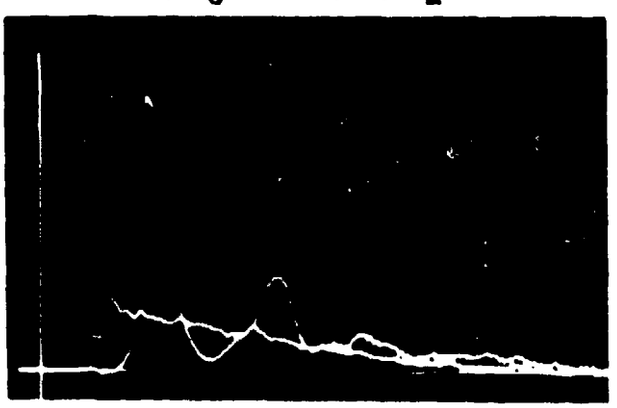

(4) 15 TK, P_o = 4.9 psi, P_m = 38.6 psi

Figure 15. Pressure variation under different layers of Kevlar swatch for a given blast loading

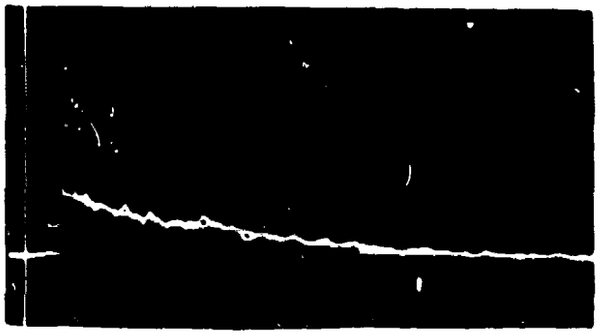

(1) 1 TB, P_o = 5.21 psi, P_m = 17.7 psi

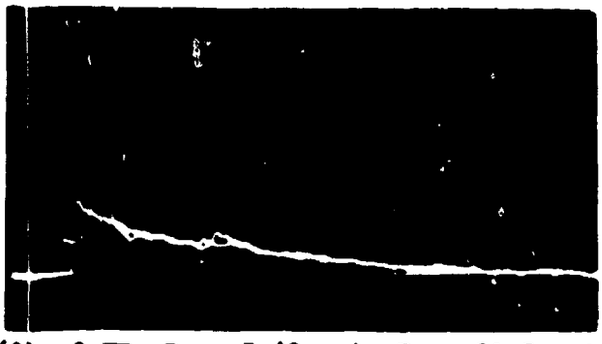

(2) 2 TB, P_o = 5.48 psi, P_m = 21.5 psi

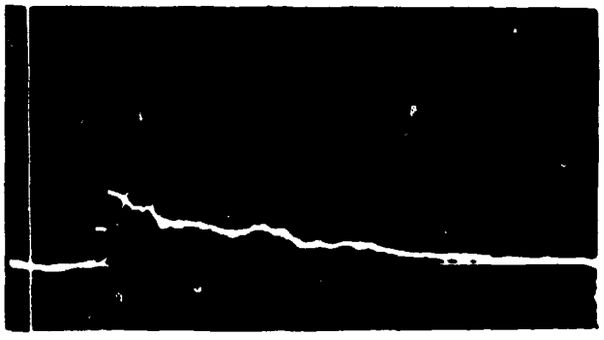

(3) 3 TB, P_o = 4.58 psi, P_m = 22.5 psi

(4) 10 TB, P_o = 4.93 psi, P_m = 25.3 psi

(5) 20 TB, P_o = 5.21 psi, P_m = 28.2 psi

(6) 25 TB, P_o = 4.66 psi, P_m = 26.9 psi

(7) 30 TB, P_o = 4.66 psi, P_m = 28.7 psi

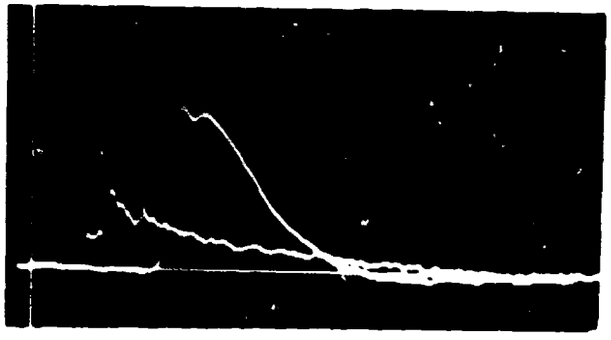

(8) 40 TB, P_o = 4.93 psi, P_m = 23.3 psi

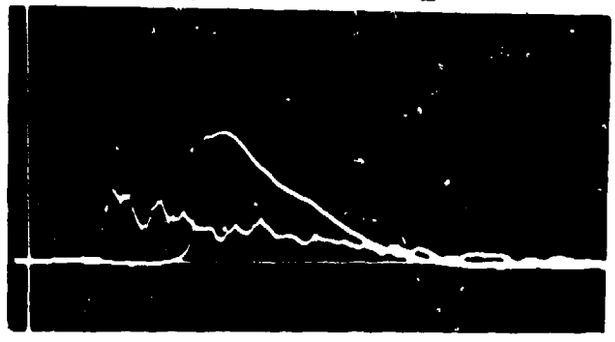

(9) 50 TB, P_o = 4.66 psi, P_m = 18.2 psi

Figure 16. Pressure variation under different layers of cloth swatch for a given blast loading

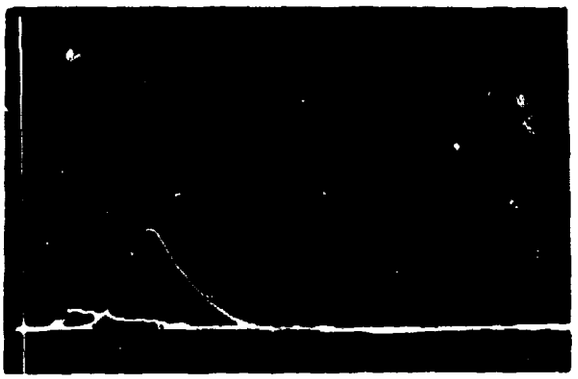

(1) P_o = 1.4 psi, P_m = 14.1 psi

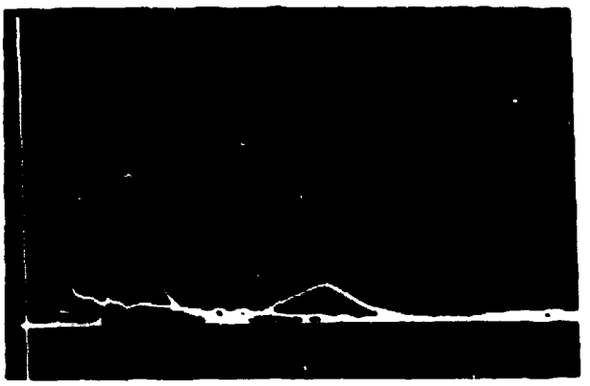

(4) P_o = 4.4 psi, P_m = 43.0 psi (Vertical scale doubled)

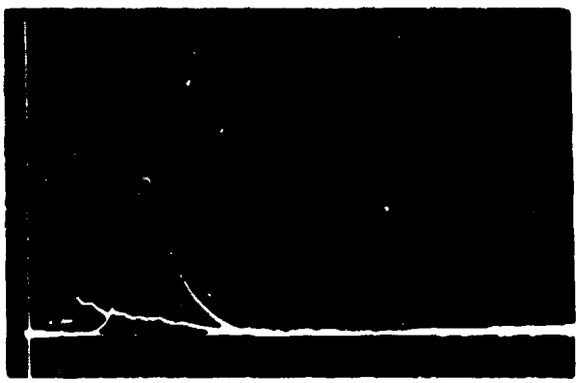

(2) P_o = 2.2 psi, P_m = 22.3 psi

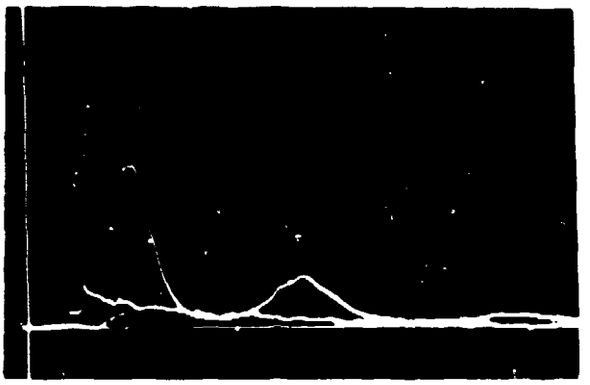

(5) P_o = 4.9 psi, P_m = 46.1 psi (Vertical scale doubled)

(3) P_o = 3.0 psi, P_m = 29.9 psi

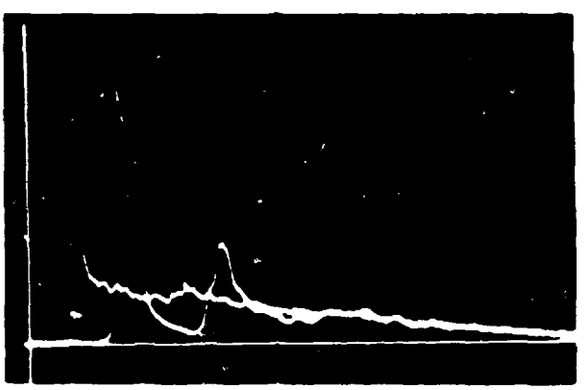

(6) P_o = 8.8 psi, P_m = 71.7 psi (Vertical scale doubled)

Figure 17. Pressure variation versus blast pressure for a 20 layer Kevlar swatch

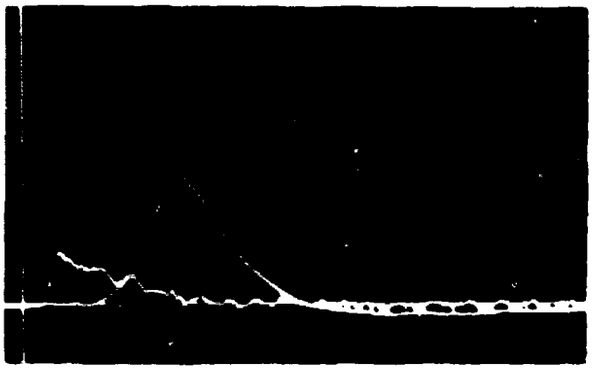

(1) P_o = 1.44 psi, P_m = 7.26 psi

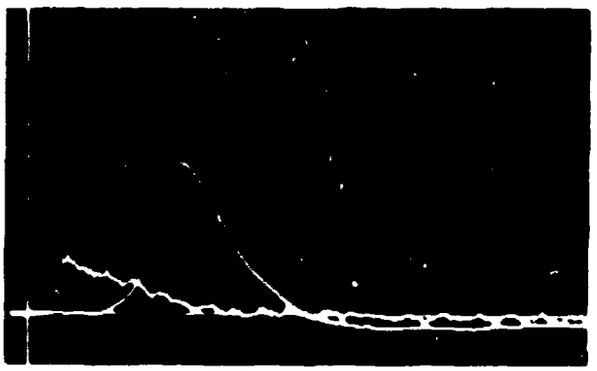

(2) P_o = 1.54 psi, P_m = 8.61 psi

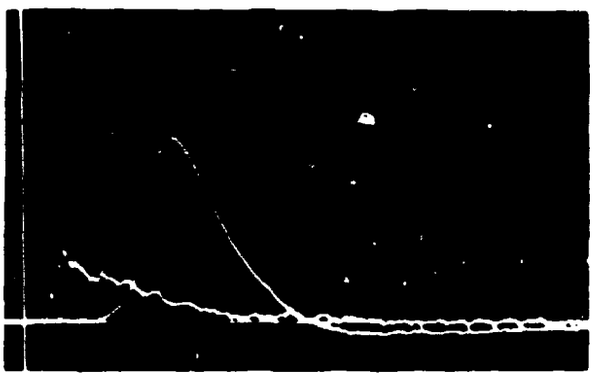

(3) P_o = 1.75 psi, P_m = 10.2 psi

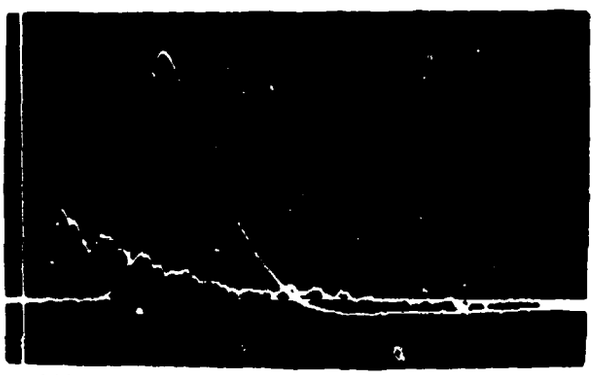

(4) P_o = 2.55 psi, P_m = 13.8 psi

(5) P_o = 3.29 psi, P_m = 17.7 psi (Vertical scale doubled)

(6) P_o = 4.66 psi, P_m = 28.7 psi (Vertical scale doubled)

(7) P_o = 6.03 psi, P_m = 36.9 psi (Vertical scale doubled)

Figure 18. Pressure variation versus input blast pressure for a 30 layer cloth swatch

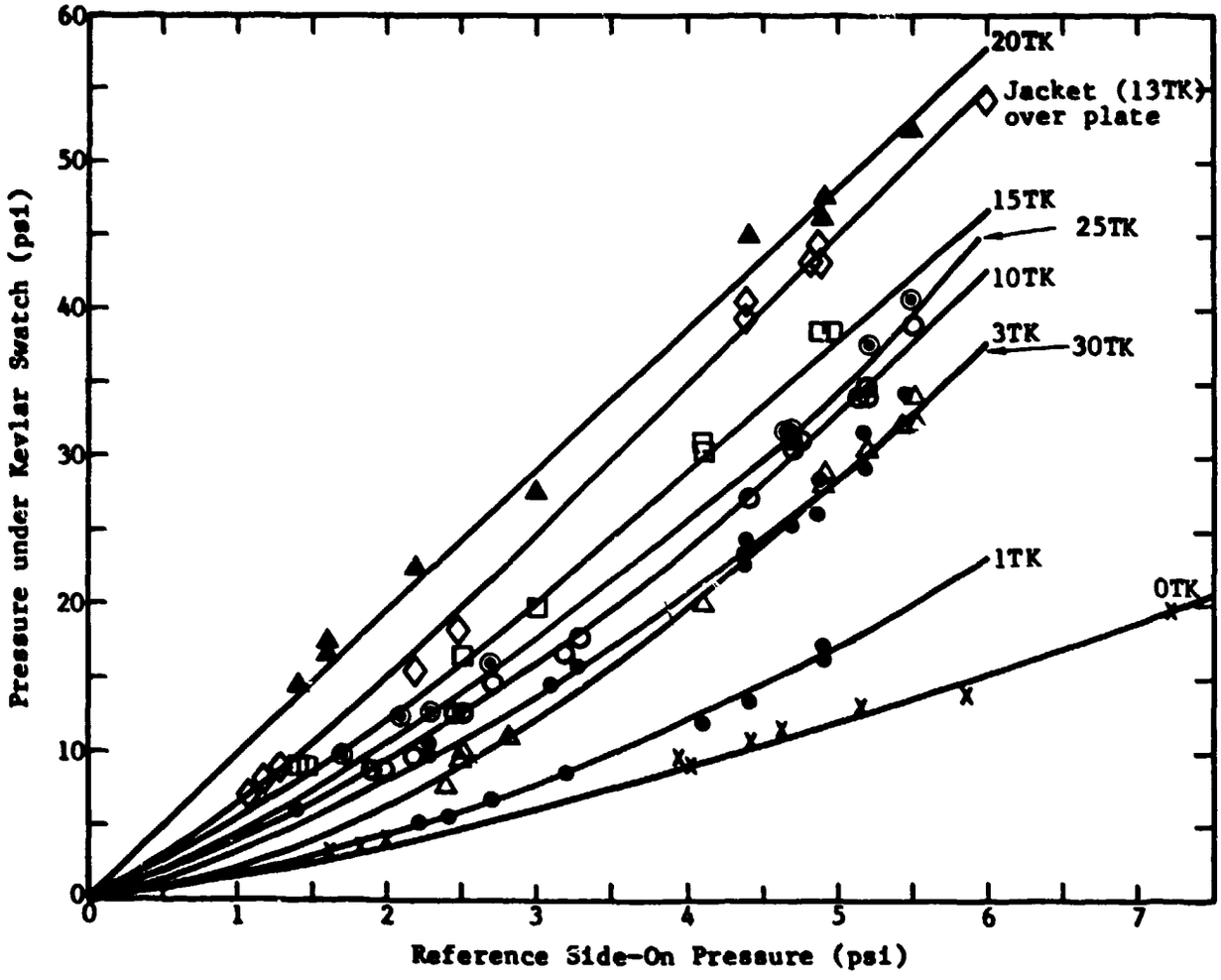

Figure 19. Pressure variation under Kevlar swatch as a function of number of layers

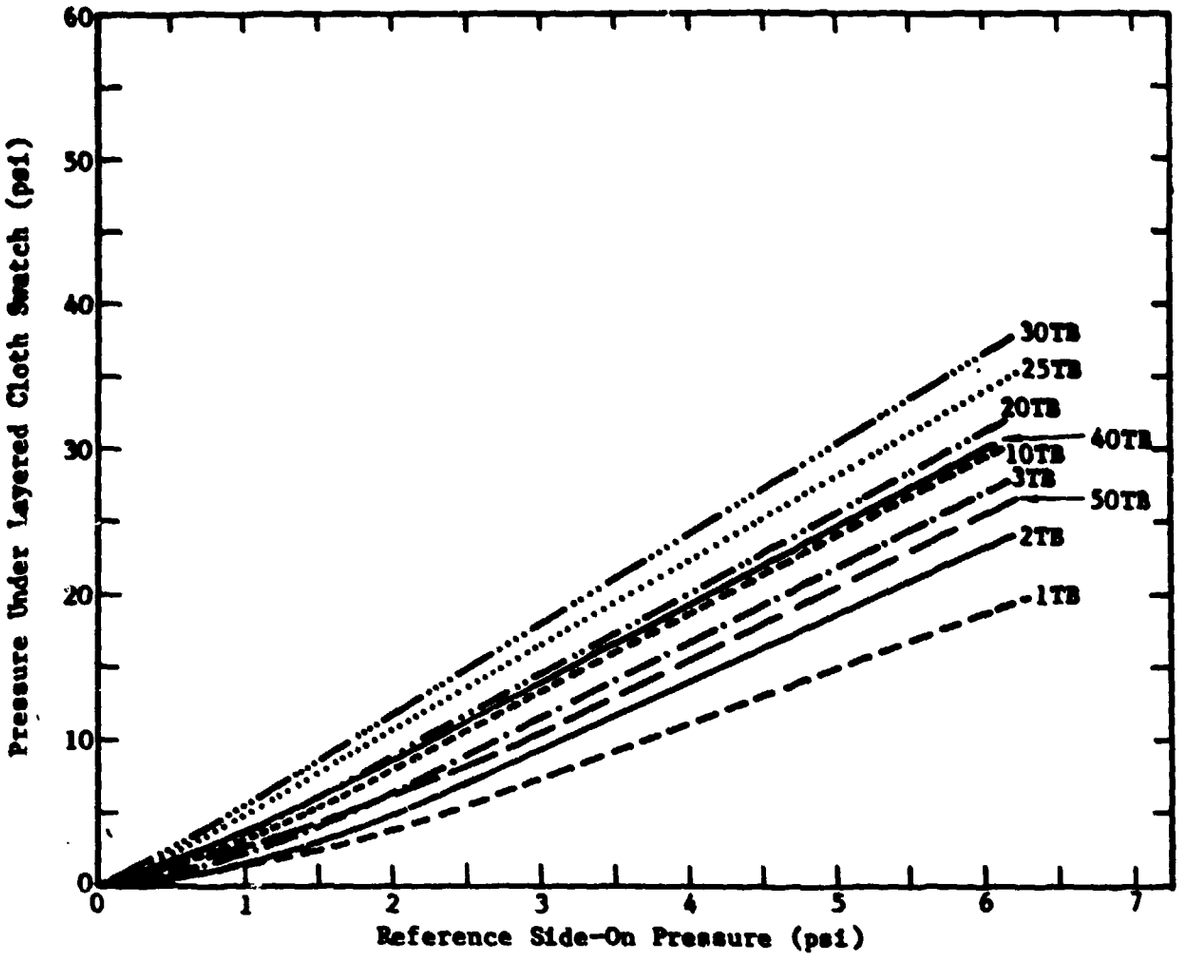

Figure 20. Pressure variation under layered cloth swatch vs side-on pressure as a function of number of layers

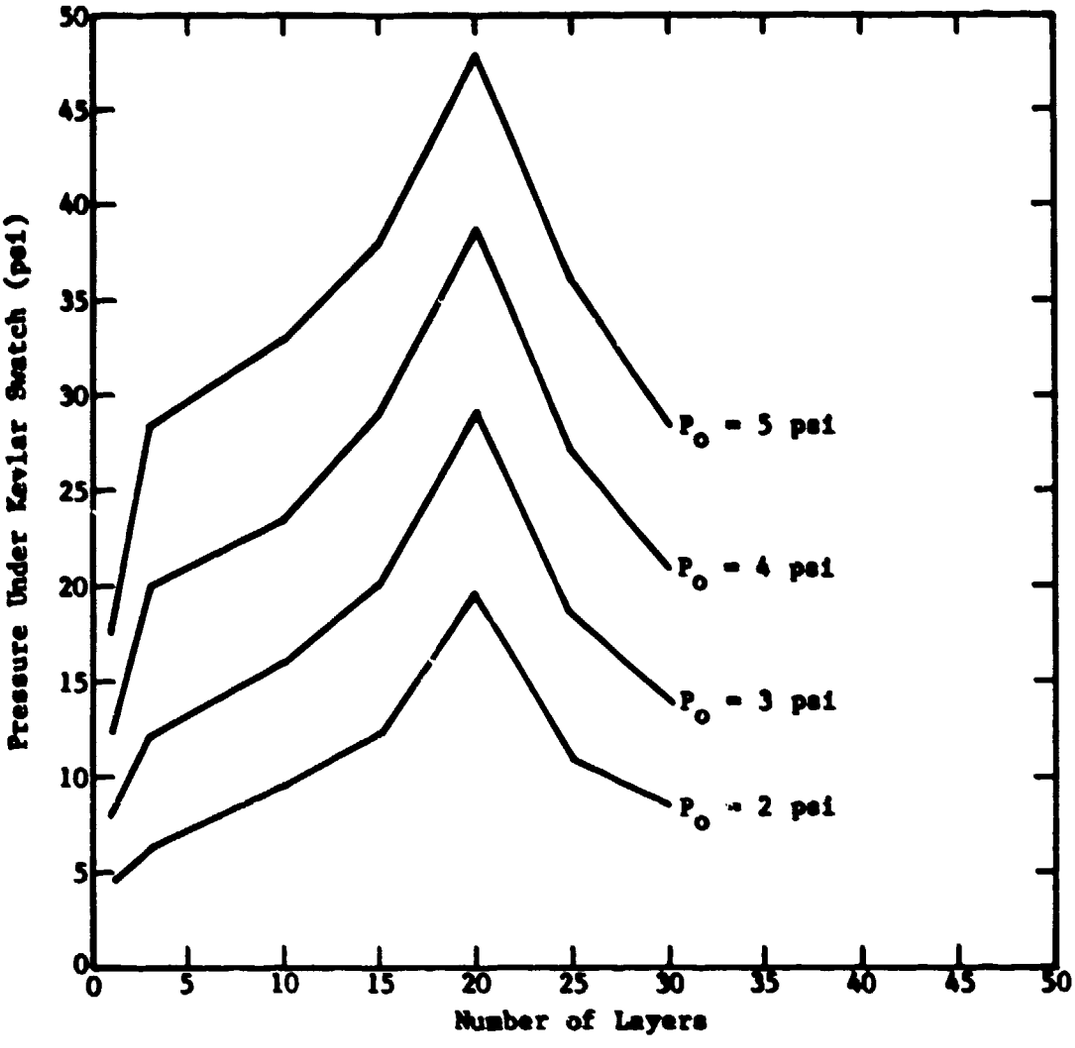

Figure 21. Pressure variation under Kevlar swatch vs number of layers for different pressure levels

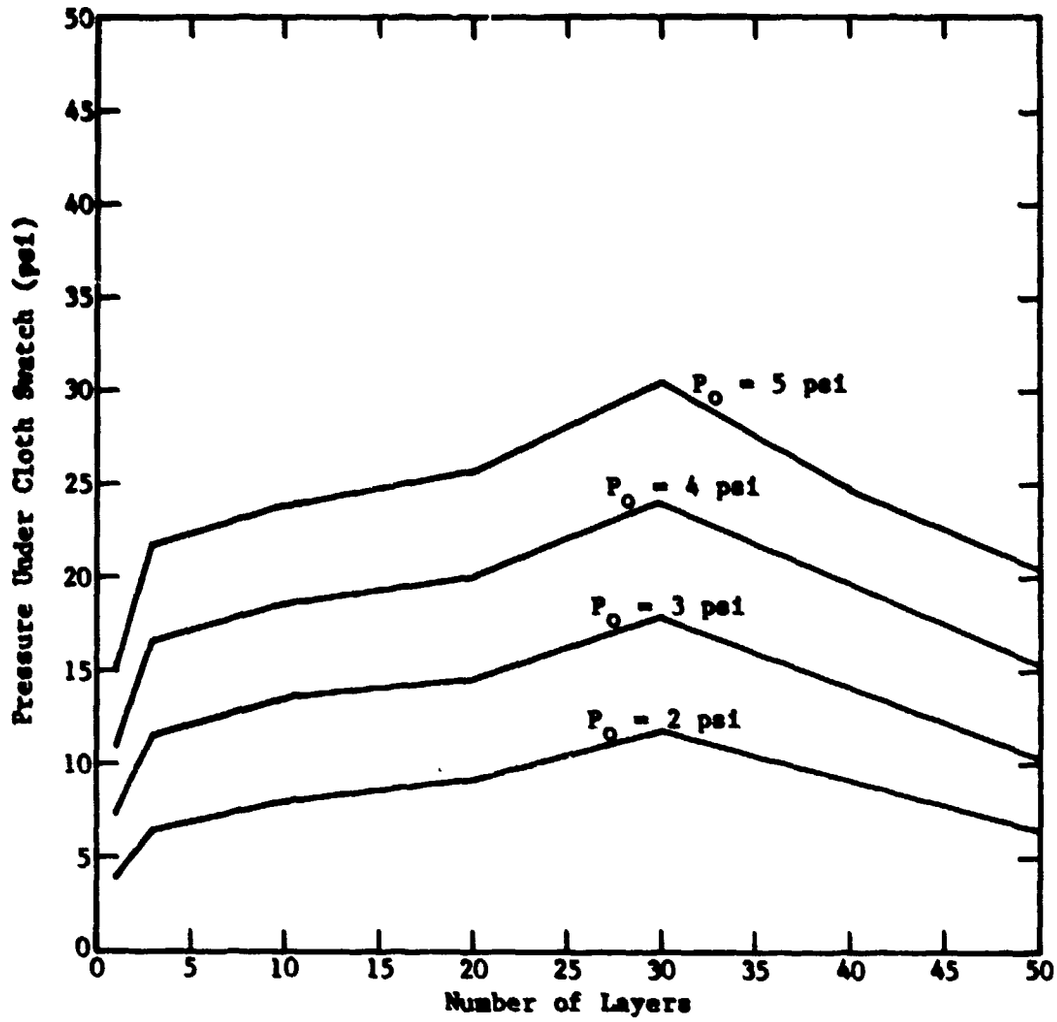

Figure 22. Pressure variation under cloth swatch vs number of layers for different pressure levels

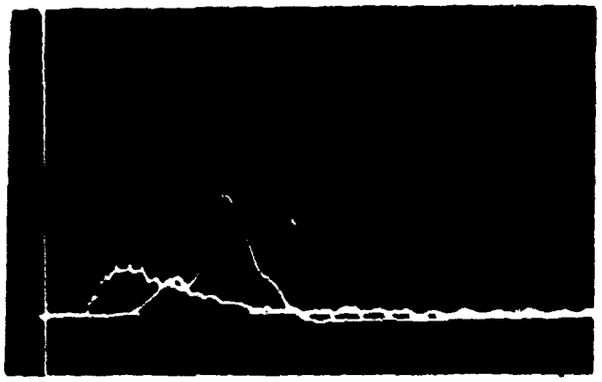

(1) P_o = 1.1 psi, P_m = 7.1 psi

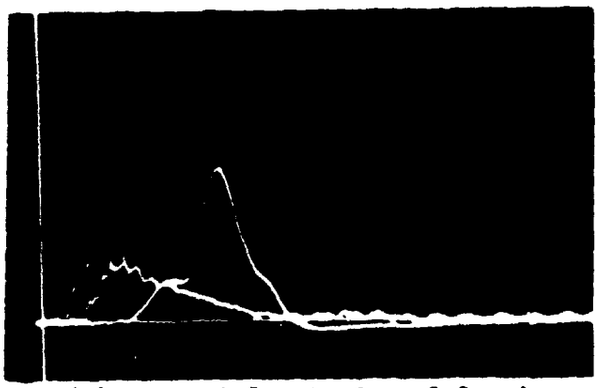

(2) P_o = 1.3 psi, P_m = 9.0 psi

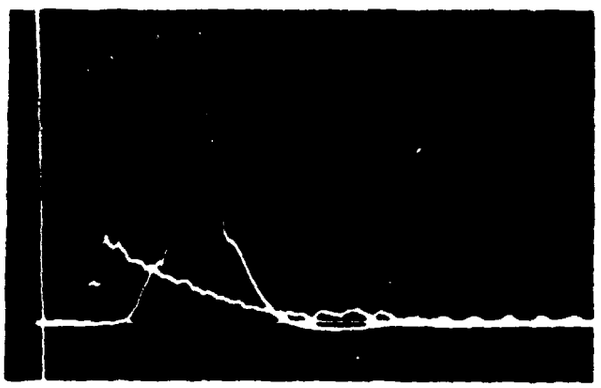

(3) P_o = 2.2 psi, P_m = 15.5 psi

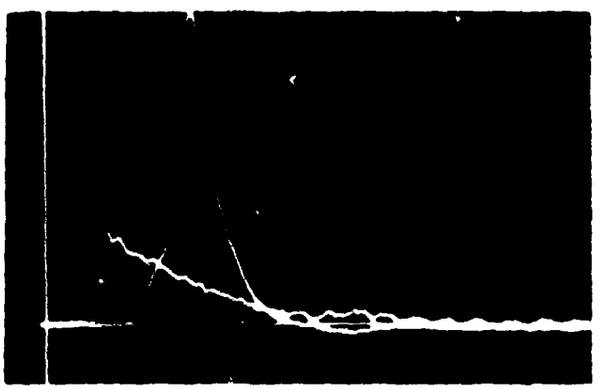

(4) P_o = 2.5 psi, P_m = 18.0 psi

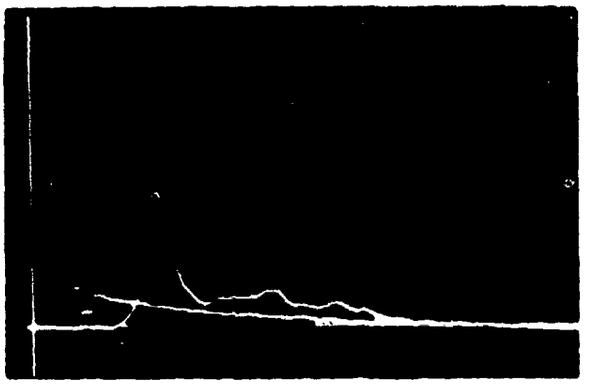

(5) P_o = 4.4 psi, P_m = 39.4 psi (Vertical scale quintupled)

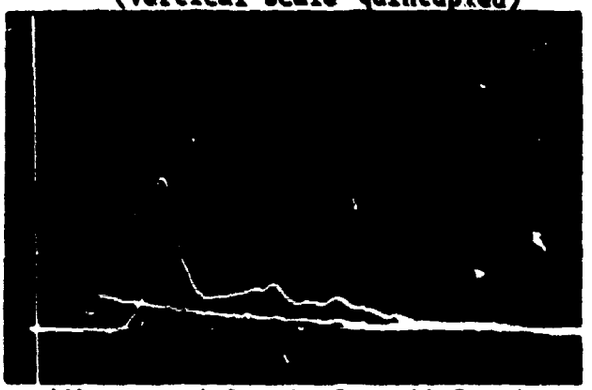

(6) P_o = 4.9 psi, P_m = 44.5 psi (Vertical scale quintupled)

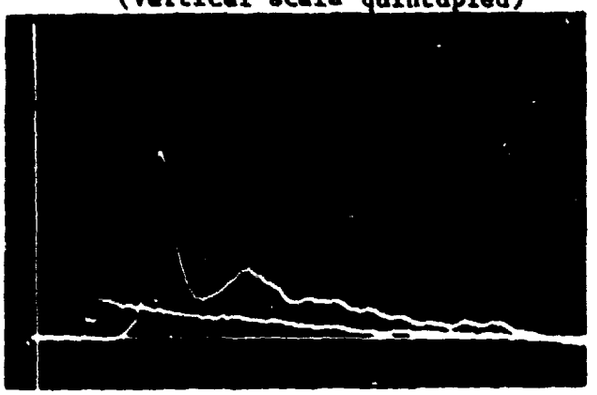

(7) P_o = 6.0 psi, P_m = 54.3 psi (Vertical scale quintupled)

Figure 23. Pressure variation versus input blast pressure as measured under a Kevlar jacket over a flat plate

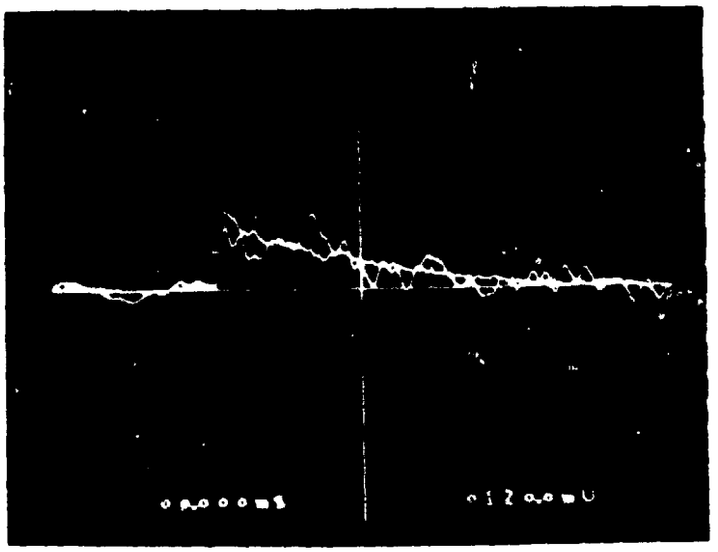

(a) Without Kevlar swatch

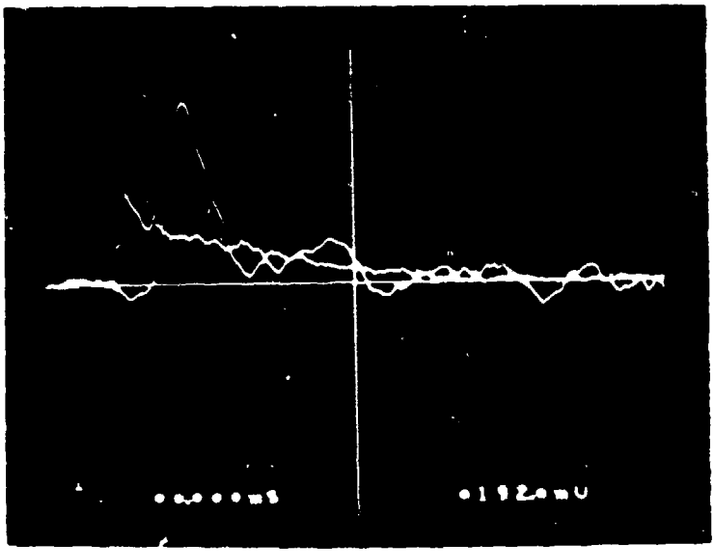

(b) With 25 layer Kevlar swatch

Figure 24. Force measurement results

covered with Kevlar fabric a much higher force was measured. As a matter of fact, the pressure calculated based on the total force and the exposed area resulted in the same pressure as that of pressure transducer measurement. The impulses evaluated based on the pressure and force transducer outputs also agreed within 10% of each other.

3.3 MANNEQUIN TEST

A major concern with respect to the swatch test was whether it could be used to represent the "whole body" effect. To study the phenomenon related to this effect, a mannequin was borrowed from the Los Alamos Laboratory at Kirtland Air Force Base.

3.3.1 Model Preparation

The mannequin was seated in an upright position and secured in a chair. A machinist's level was installed on top of the mannequin's head to serve as a reference for upright position. A bushing threaded into the chest plate was used for mounting the pressure transducer. The extra length of the bushing allowed the mounted transducer to be flush with the torso model surface. Figure 25 shows the location of the pressure transducer and the bare mannequin test setup.

The Kevlar jacket came with a Velcro flap in the front. This provision allowed the jacket to be fitted snugly over the mannequin. During the test, ample silicone grease was applied over the transducer surface to ensure proper pressure transfer from the jacket to the transducer. Figure 26 shows the test arrangement with the mannequin covered with the PASGT vest.

To test the effect of clothing, a T-shirt and a lab coat were worn under the Kevlar jacket as shown in Figure 27.

3.3.2 Mannequin Test Results

Figures 28 through 31 show the results of the mannequin tests under the above mentioned test conditions. For convenience of comparison, all signals used the same pressure scales.

Figure 25. Pressure measurement on bare mannequin

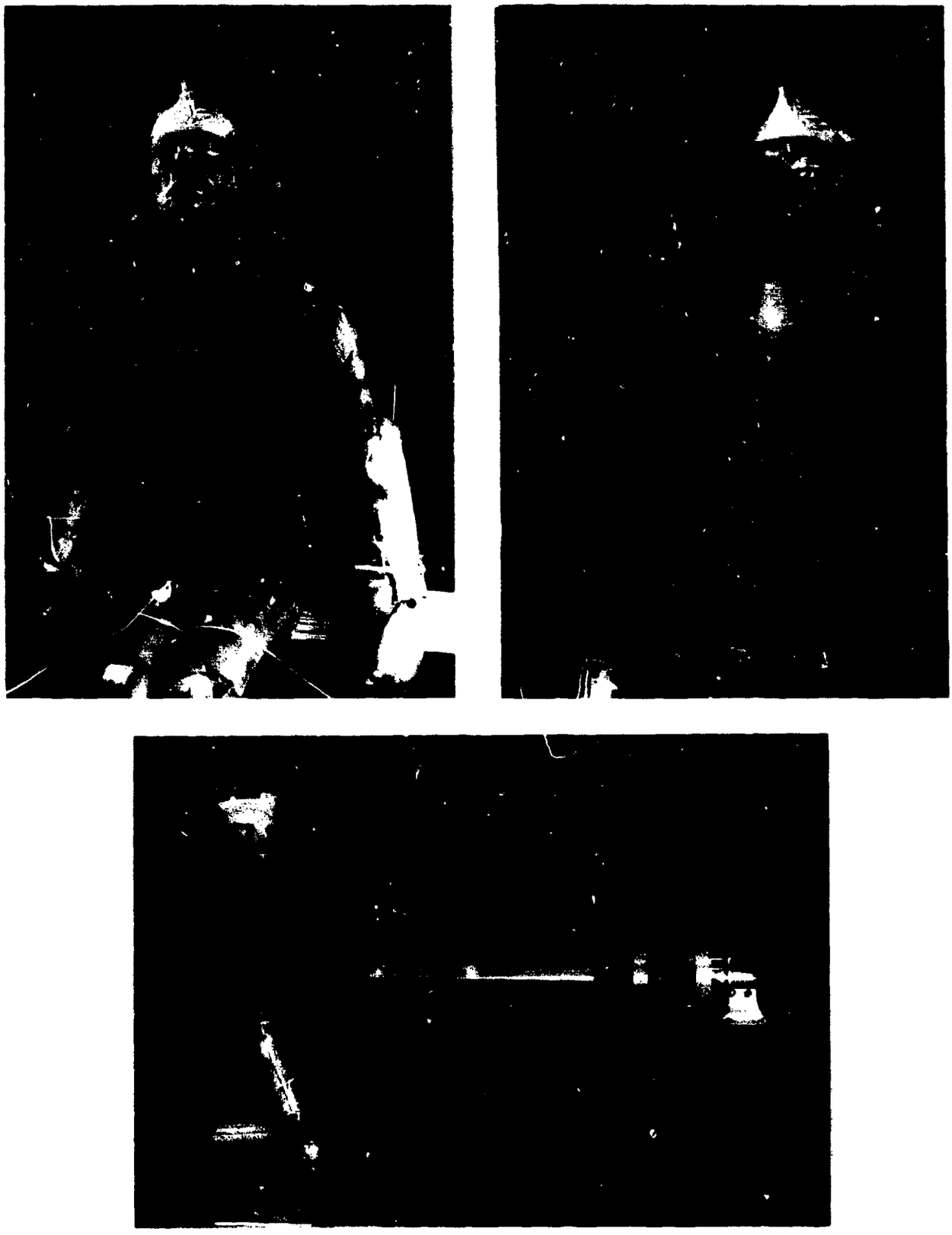

Figure 26. Pressure measurement on mannequin with Kevlar jacket

Figure 27. Pressure measurement on mannequin. A lab coat and a T-shirt are shown under the Kevlar jacket.

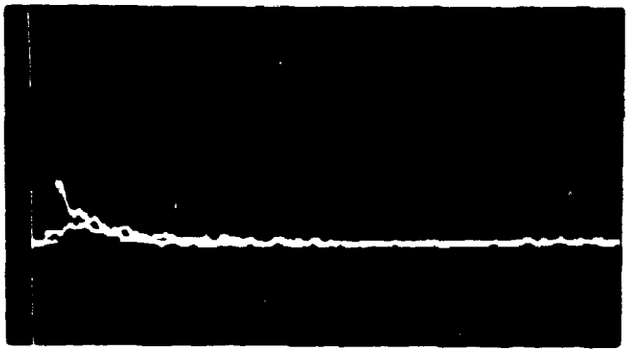

(1) P_o = 2.19 psi, P_m = 9.21 psi

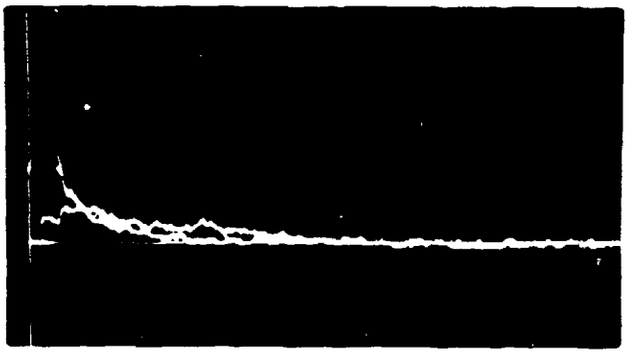

(2) P_o = 3.29 psi, P_m = 13.3 psi

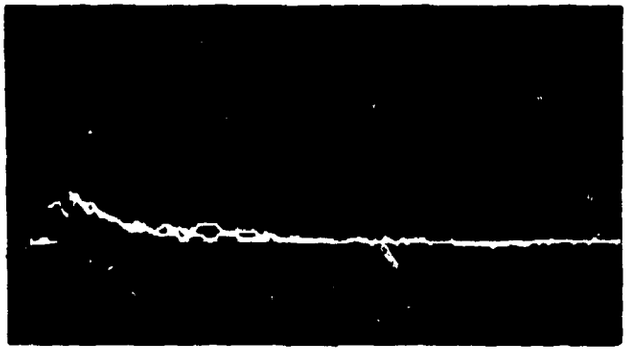

(3) P_o = 3.84 psi, P_m = 15.4 psi

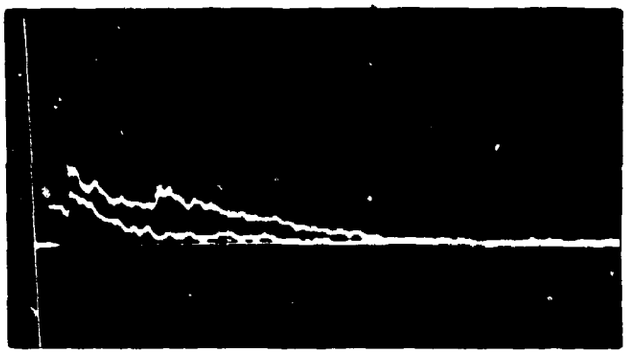

(4) P_o = 6.03 psi, P_m = 27.1 psi

Figure 28. Pressure variation measured on bare mannequin

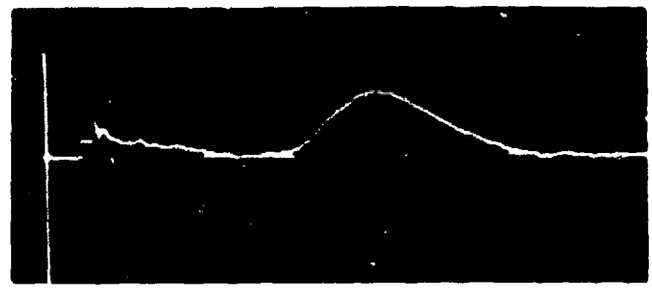

(1) P_o = 4.67 psi, P_m = 35.8 psi

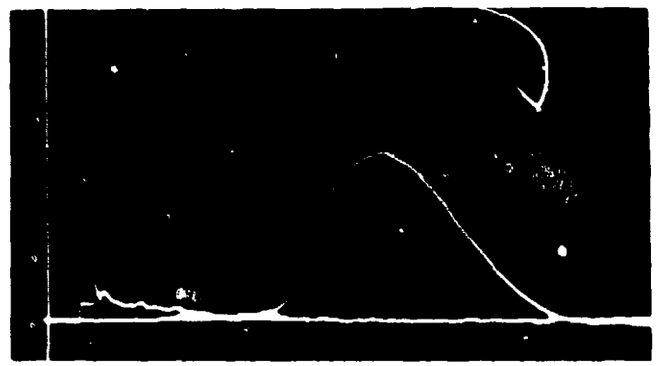

(2) P_o = 5.21 psi, P_m = 47.1 psi

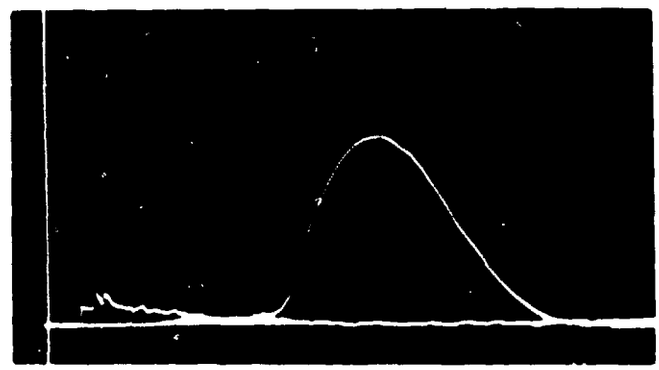

(3) P_o = 5.48 psi, P_m = 52.2 psi

(4) P_o = 6.03 psi, P_m = 57.3 psi

Figure 29. Pressure variation measured under Kevlar jacket

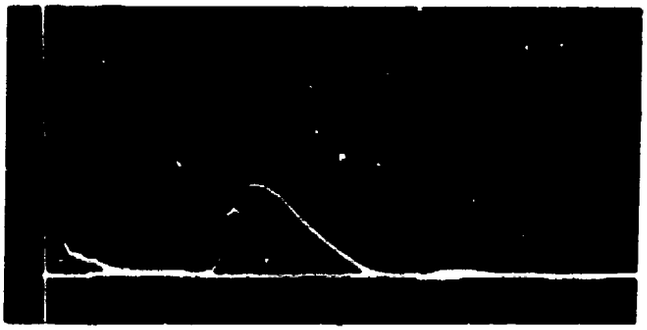

(1) P_o = 4.39 psi, P_m = 25.1 psi

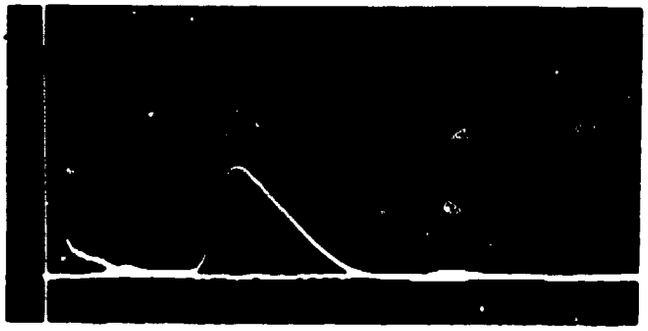

(2) P_o = 4.93 psi, P_m = 30.2 psi

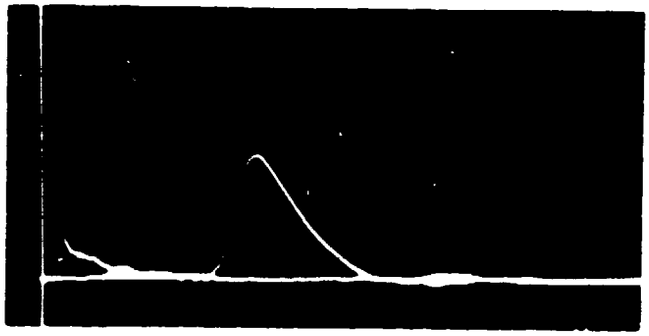

(3) P_o = 5.48 psi, P_m = 34.3 psi

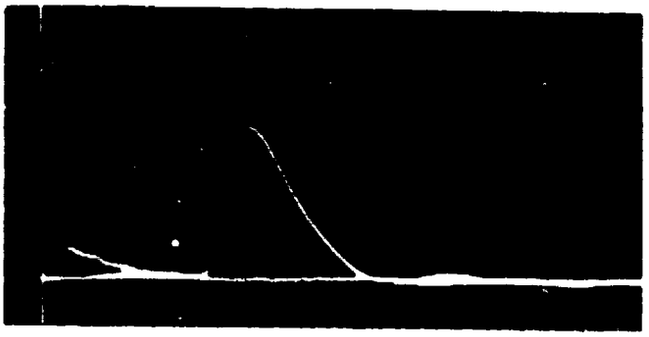

(4) P_o = 6.03 psi, P_m = 42.5 psi

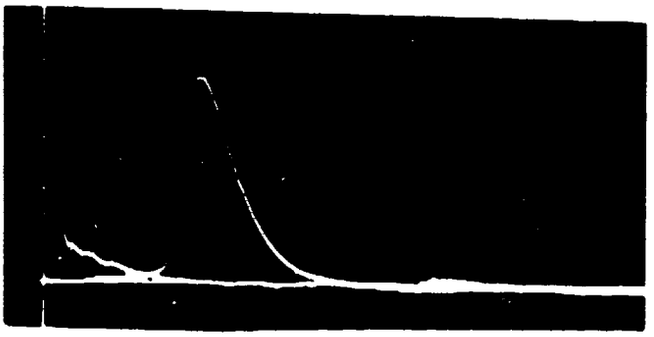

(5) P_o = 7.68 psi, P_m = 56.8 psi

Figure 30. Pressure variation measured on a mannequin; a lab coat and a T-shirt were worn under the Kevlar jacket (time scale was doubled)

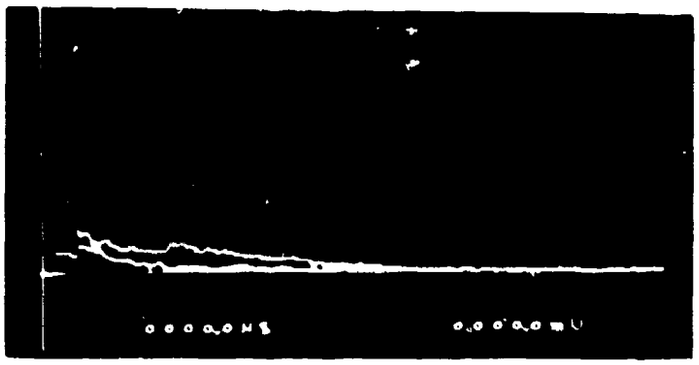

(a) Bare

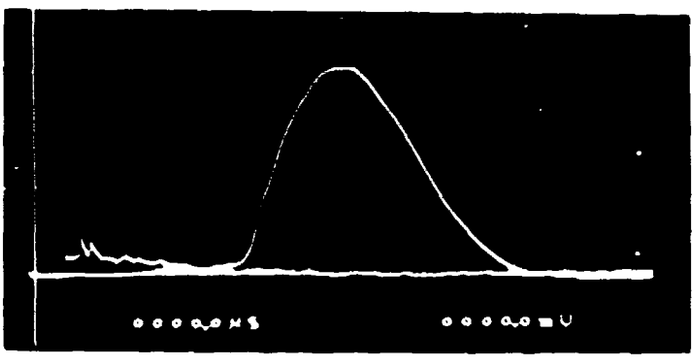

(b) Under Kevlar jacket

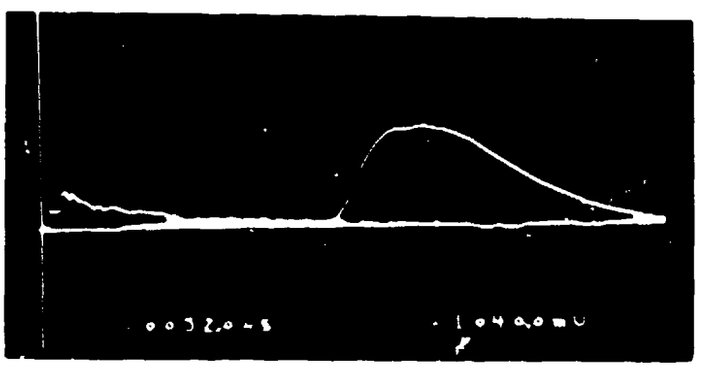

(c) Under Kevlar jacket, lab coat and t-shirt

Figure 31. Pressure measurement on mannequin

As shown in Figure 28, the bare mannequin test results show the familiar face-on pressure signals. The measured pressure (p_m) increases with the reference input blast signal (p_o).

Figure 29 shows the result measured under the PASGT vest. The measured pressures show that they were significantly amplified and delayed as compared to the bare mannequin tests. Furthermore, the pressure signals had much longer durations.

Figure 30 shows the result for the case when a T-shirt and a lab coat were worn under the PASGT vest. The signals were not amplified as much as in the case when the jacket had perfect contact with the chest wall. We believe that the decrease in magnitude was probably due to the relatively poor coupling between the different types of fabrics. Thus, instead of enhancing the pressure, these added layers appear to dissipate part of the energy.

Figure 31 compares the pressure signals for the three different kinds of test conditions. The results of this series of tests is summarized in Figure 32. The consistently lower values for the case when additional clothing was worn under the vest implies that coupling among different fabrics may not be as effective as a single sewn layered material.

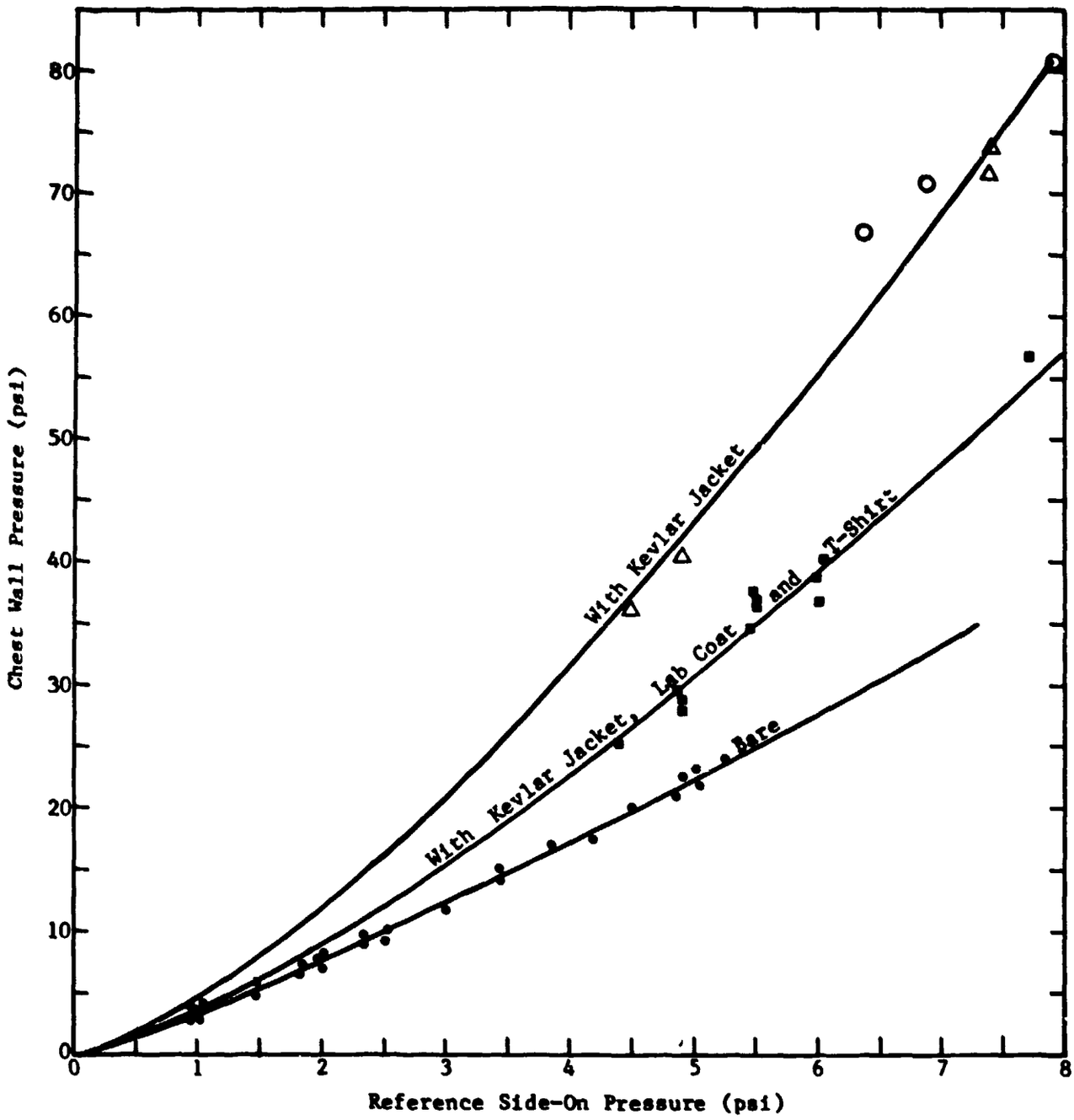

Figure 32. Effect of Kevlar jacket on mannequin chest wall pressure

4. ONE DIMENSIONAL MODEL OF THE LUNG AND CHEST WALL COMPOSITE STRUCTURE

4.1 INTRODUCTION

The high pressure observed under the Kevlar swatches may account for the higher ITP seen when layered clothing was worn. A more direct test of this observation would be to measure the net effect in a model. A key element in this approach was the selection of the modeling material. In this section, approaches to material selection and the findings from pertinent experiments are presented. The one dimensional model was then fabricated from the selected materials and used for both pressure and accelerometer measurements.

4.2 LUNG AND CHEST WALL MODEL MATERIAL SELECTION

In order to achieve a realistic representation of the lung and chest wall model, the selected material must have properties similar to real tissue. There are many physical and biological properties for each tissue. It is unlikely that all the properties can be represented simultaneously by a single model material without resorting to the exact tissue itself. On the other hand, among all tissue properties the most important were the wave transfer characteristics. This argument was born out of analytical results and field observation experience that wave motion was the fundamental mechanism of lung injury. The material selection was therefore based solely on wave propagation speed.

A number of candidate materials were screened and selected based on their texture and construction. These materials were then measured accurately to determine their respective wave speeds. Based on the findings of Yen and Fung, the wave speed of lung tissue is in the range 25-70 m/sec while that of the chest wall was greater than 1000 m/sec (See Table 2 and Fig. 33). Preliminary tests indicated that certain types of spongy material and hard rubber had properties close to these values. They were used for subsequent tests.

Table 2. Velocity of Sound in Various Tissues, Air and Water*

Tissue	Velocity of Sound (m/sec)	Density (g/cm^3)	Reference
Muscle	1580	1	Ludwig (1950), Frucht (1953) (1953), von Gierke (1964)
Fat	1450	1	Ludwig (1950), Frucht (1953)
Bone	3500	2.0	Clemedson & Jönsson (1961)
Ribs and intercostal muscle	<1000		Clemedson & Jönsson (1961)
Collapsed lung	650 (ultrasound)	0.4	Dunn & Fry (1961)
Collapsed lung, pneumonitis	320 (ultrasound)	0.8	Dunn & Fry (1961)
Lung, air filled, horse	25	0.6	Rice (1983)
Lung, air filled, horse	70	0.125	Rice (1983)
Lung, air filled, calf	24-30		Clemedson & Jönsson (1962)
Air	340		Dunn & Fry (1961)
Water, distilled, 0°C	1407		Kaye & Laby (1960)
Air bubbles (45% by vol.) in glycerol and water	20		Campbell & Pitcher (1958)

*From "Speed of Stress Wave Propagation in the Lung," by M. R. Yen, Y. C. Fung, H. H. Ho, and G. Butterman.

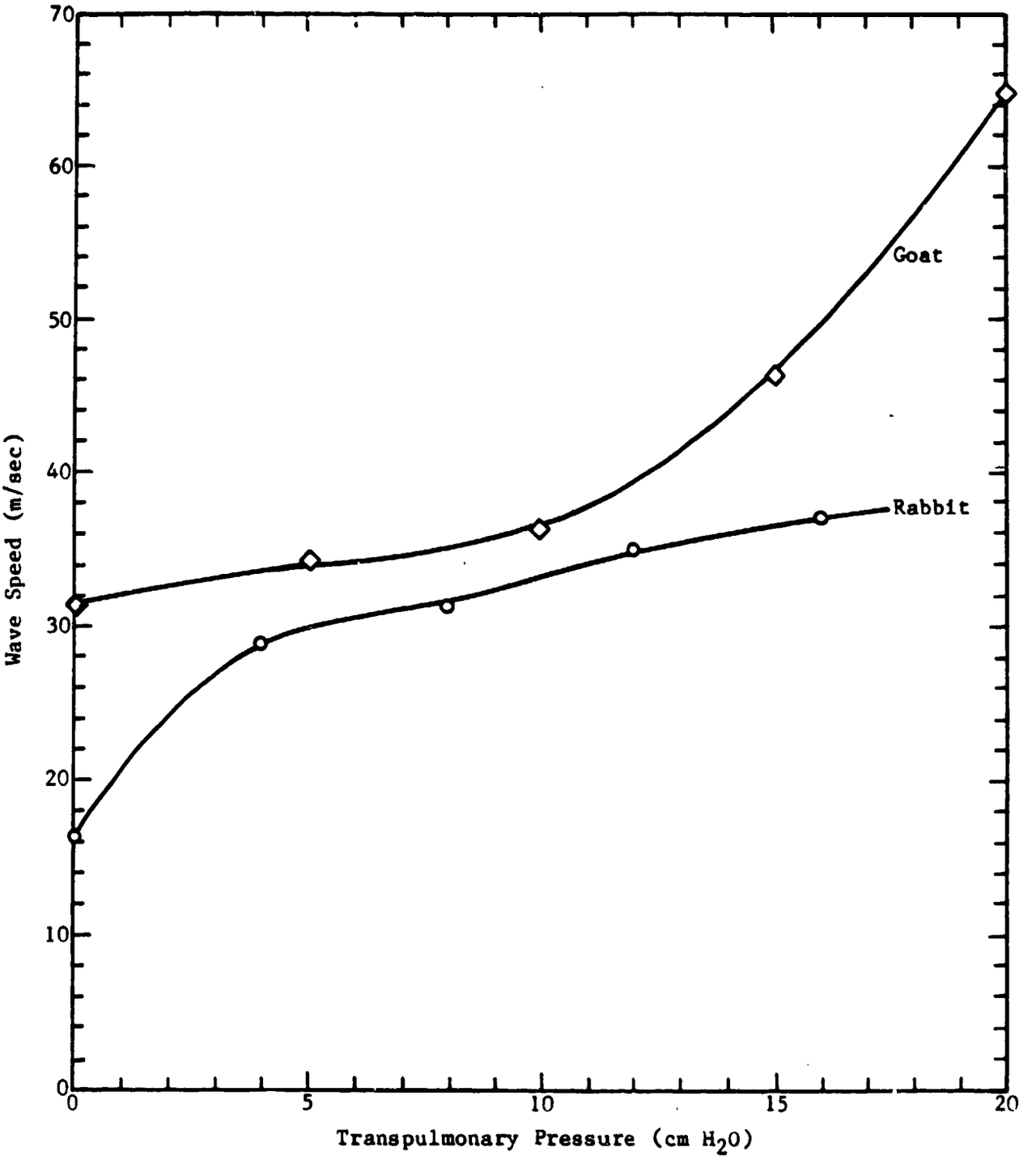

Figure 33. Velocity of wave in lung as measured by Fung and Yen

Initially, the wave speed was measured directly by exposing the test material to the blast signal and measuring the time delay between the rise times of two pressure signals. These pressure signals were obtained from two pressure transducers: one directly under the test material, and the other installed next to the material but flush with its surface. In this way the extra time required for the pressure to reach the second transducer would represent the time required to travel through the test sample. Since the test material thickness was known, the wave speed of the test material could be calculated.

The signals obtained by exposing the test sample directly to the whole shock were found to be noisy and inconsistent. They also varied with the magnitude of the blast signal - a stronger shock tends to have a higher wave speed than that of a weaker shock. A modified approach was therefore adopted. In this case, two 1/8 in. holes were drilled in an end plate on the shock tube: one hole directly facing the test sample and the other facing the reference pressure transducer. Since the blast signals coming through these holes were significantly restricted, relatively weak signals impinged on the target. The measured pressures under this arrangement were found to be much cleaner and the measured time delays were more consistent.

An alternative approach of wave speed measurement was to mount the test material on a small, water-filled chamber. One transducer was mounted at the opposite end of the chamber and a reference transducer was mounted flush with the sample surface adjacent to the test sample (see Fig. 34). Since the wave speed in water was well known, the wave speed through the material covering the front face of the water chamber could then be calculated once the total travel time was known. Again, the start time was provided by the reference pressure transducer.

Typical pressure time histories using each approach are shown in Figures 35 and 36. The latter has slightly better defined start points in the time traces, but the results agree well.

Based on this series of tests, two materials - namely the closed-cell, double-skin neoprene and the hard rubber sheet - were found to have wave speeds of 50 and 1065 m/sec, respectively. The values were close to those of

Figure 34. Water chamber used for wave speed measurement. The material to be tested is shown directly over the water surface.

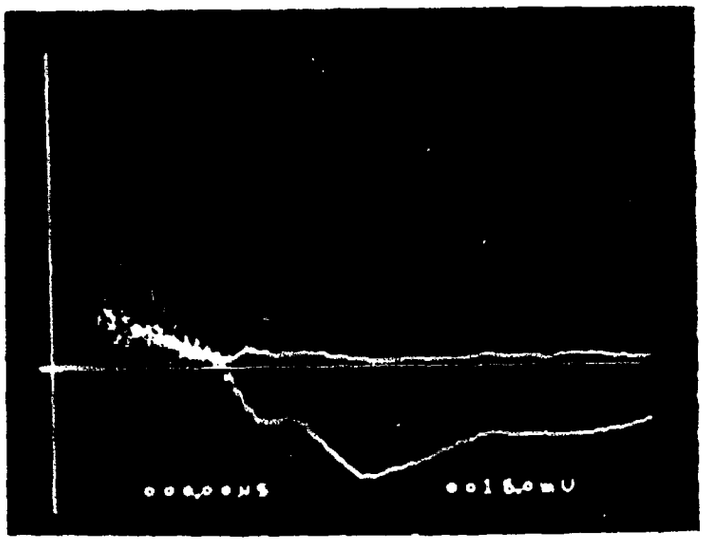

(a) Pressure traces for wave speed measurements

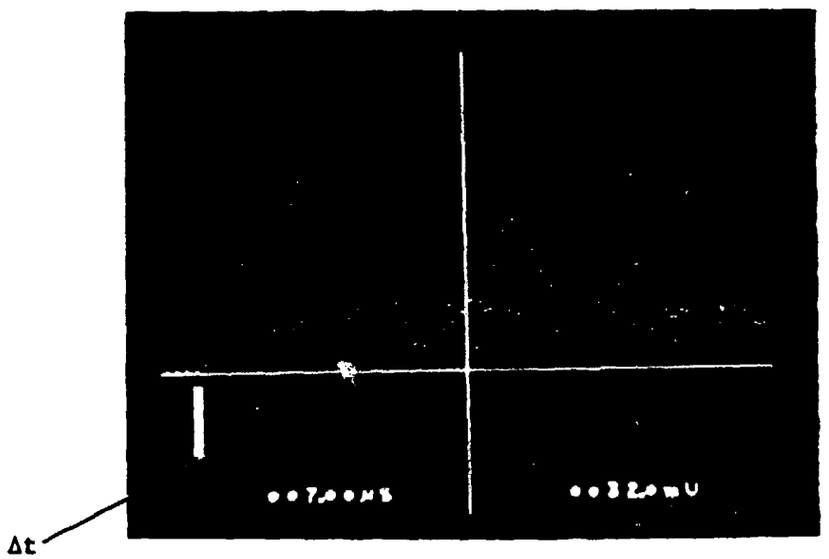

(b) Signals greatly expanded in time for better resolution

Figure 35. Pressure traces for wave speed measurements

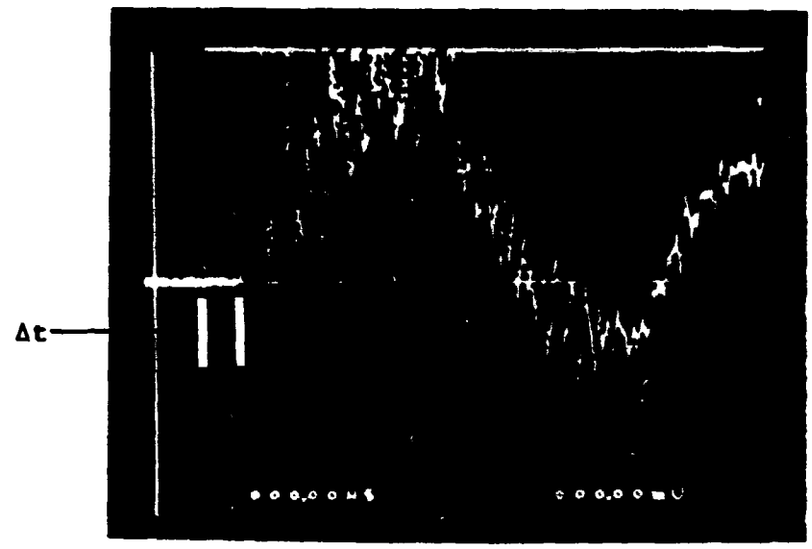

(a) Time delay measured between reference surface transducer and that directly under test material

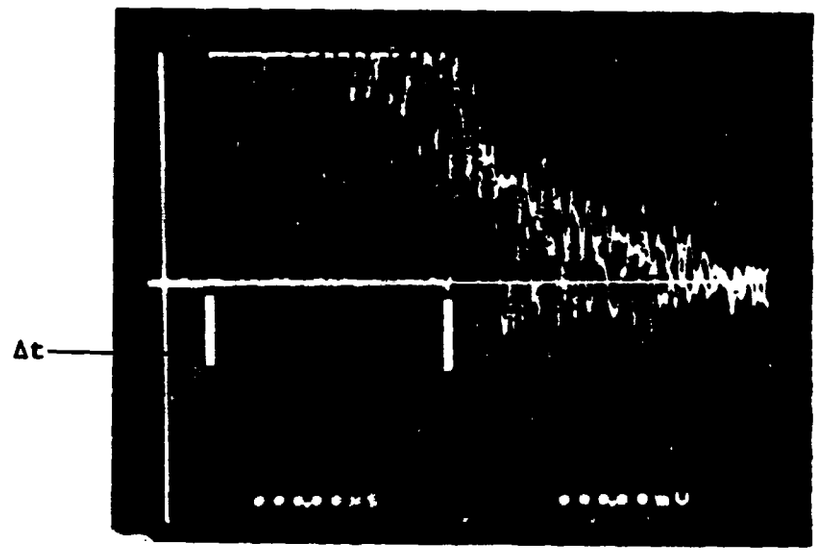

(b) Time delay measurement when a water chamber is used

Figure 36. Wave speed measurements with and without auxiliary water chamber

actual lung tissue and chest wall. They were chosen for subsequent one dimensional ITP and acceleration tests.

The test sample was constructed with 0.75 inch hard rubber "muscle" and 2.25 inch neoprene foam "lung" to simulate the dimensions of a typical cross section of the upper torso.

4.3 INTRATHORACIC PRESSURE MEASUREMENTS

The one dimensional lung and chest wall model described above was mounted on the target plate for blast tests. The results for both Kevlar covered and uncovered conditions were measured as in the swatch tests.

Since the test model protruded 3 inches from the mounting plate, it would interfere with the side wall pressure measurement when the same mounting arrangement as the swatch tests was used. For this series of tests, therefore, an end plate with a 2 inch diameter hole at the middle was used to allow the passage of the blast pressure. The 1-D model was then mounted on a support with its surface flush with the end plate and directly facing the exit hole.

Figure 37 shows examples of measured pressures with and without Kevlar swatch coverages. These signals were taken using the same reference pressures. Note that, instead of higher values, the pressures under the test model for both cases are smaller than the reference pressures. The Kevlar swatch does not appear to have any noticeable effect. Results for various input blasts are summarized in Figure 38 for both taped and untaped test conditions. As shown, when the model was taped around its sides and secured to the target plate, the reinforcing effect of the tape would cause further reduction in the measured pressures, perhaps due to the stiffening effect of the tape.

The reduced magnitudes obtained under the test sample indicated that there was a strong dissipative effect of the thick composite material. The overwhelming dissipative effect of the torso wall model was probably the reason why there was no noticeable difference between the results with and without Kevlar swatch coverage.

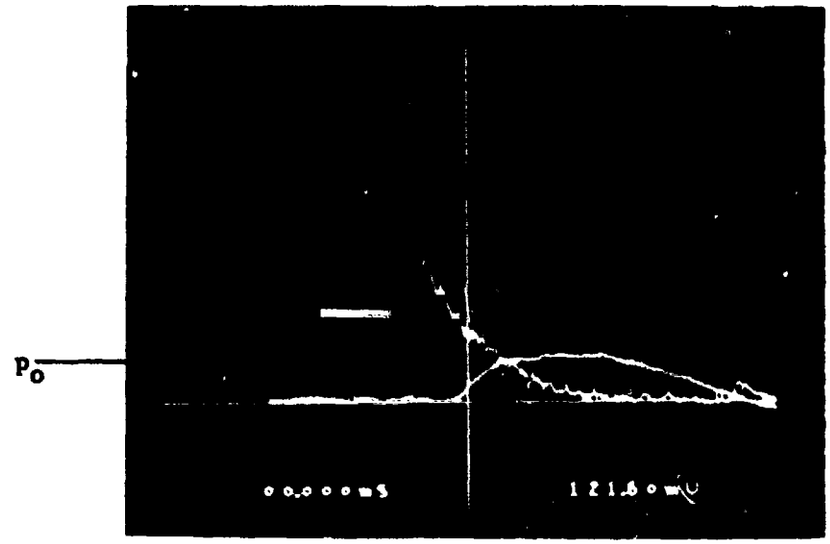

(a) Without Kevlar swatch covering

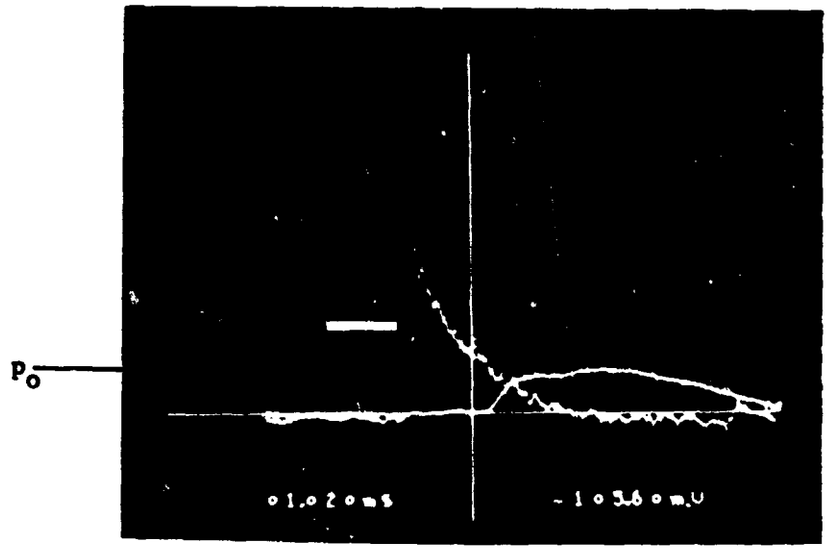

(b) With covering

Figure 37. Pressure trace under a one-dimensional lung and chest wall model

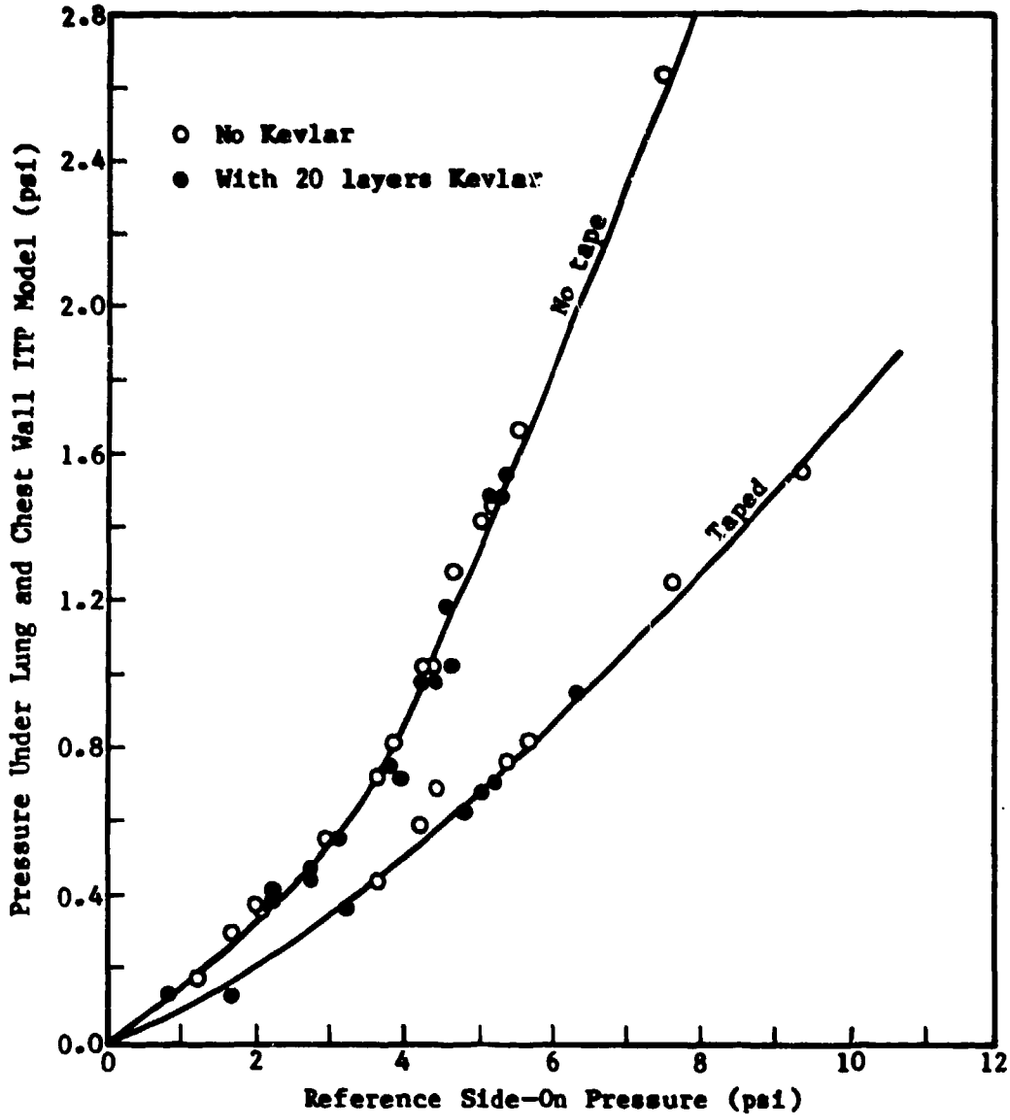

Figure 38. Effect of Kevlar fabric on pressure signal under lung and chest wall model material

4.4 ACCELERATION MEASUREMENT

In addition to the pressure measurements, acceleration at the composite model surface was measured with an accelerometer. Because of its small mass and direct blast exposure, initial tests showed that the acceleration signal would be significantly masked by the blast noise. Subsequent tests were therefore conducted with the accelerometer covered with a small shell to shield the blast noise.

Figure 39 shows the arrangements of the accelerometer installation for the test conditions with and without Kevlar swatch. The peak accelerations for both cases were plotted against the reference wall pressure as shown in Figure 40. Note that the chest wall peak acceleration was substantially reduced when it was covered with the Kevlar swatch. Since the Kevlar swatch was well bonded to the model surface, the reduced peak acceleration when the Kevlar swatch was present showed that it slowed down the accelerometer response.

Figure 41 shows an example of the signals of the pressure and the acceleration when the Kevlar swatch was mounted directly against a target plate without the one dimensional torso wall model. The pressure transducer was mounted on the target plate directly under the swatch and the accelerometer over the swatch. The figure shows that the measured pressure corresponds directly with the movement of the Kevlar swatch.

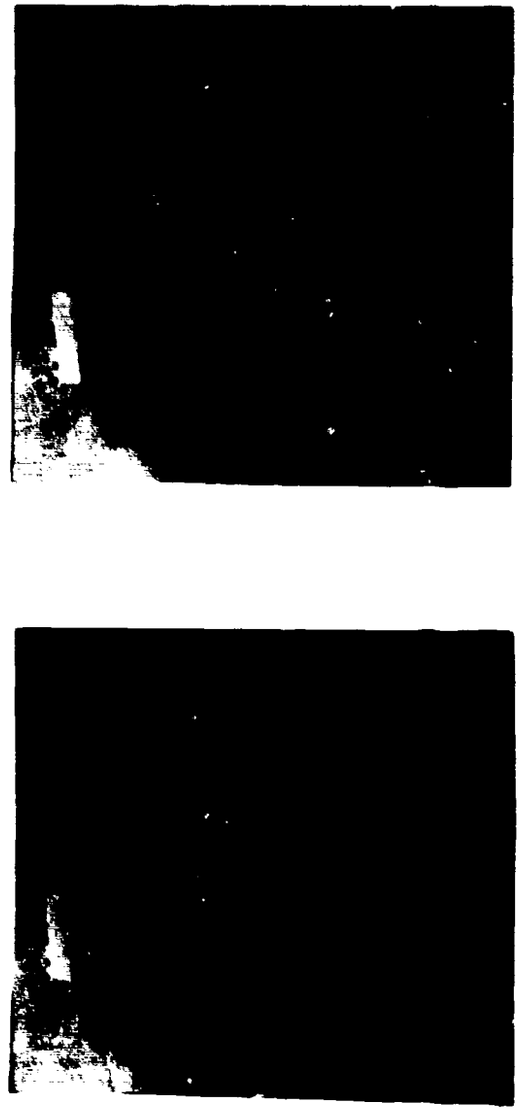

Figure 39. Accelerometer measurement installations

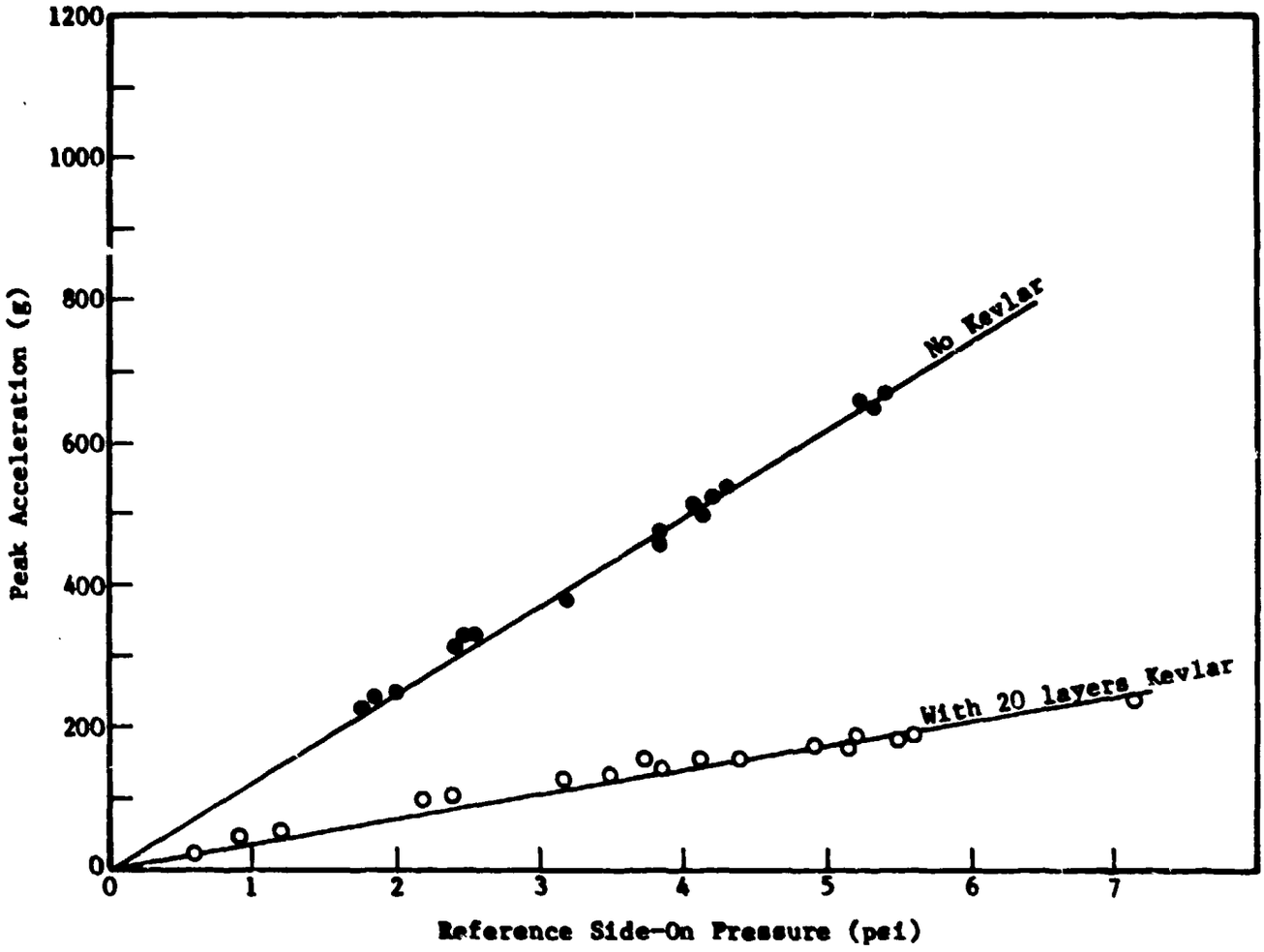

Figure 40. Effect of Kevlar swatch on chest wall acceleration

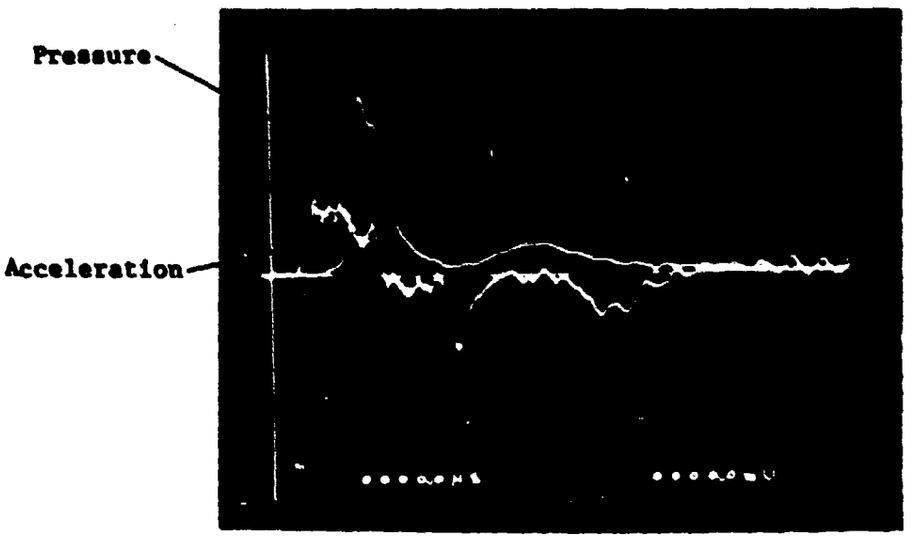

Figure 41. Pressure trace under Kevlar swatch vs swatch surface acceleration

DISTRIBUTION LIST

12 copies	Director Walter Reed Army Institute of Research Walter Reed Army Medical Center ATTN: SGRD-UWZ-C Washington, DC 20307-5100
1 copy	Commander US Army Medical Research and Development Command ATTN: SGRD-RMI-S Fort Detrick, Frederick, MD 21701-5012
12 copies	Defense Technical Information Center (DTIC) ATTN: DTIC-DDAC Cameron Station Alexandria, VA 22304-6145
1 copy	Dean School of Medicine Uniformed Services University of the Health Sciences 4301 Jones Bridge Road Bethesda, MD 20814-4799
1 copy	Commandant Academy of Health Sciences, US Army ATTN: AHS-CDM Fort Sam Houston, TX 78234-6100